NASA CR-72734
PWA FR-3790

INTERIM REPORT

90-DEGREE SECTOR DEVELOPMENT OF A SHORT LENGTH COMBUSTOR FOR A SUPERSONIC CRUISE TURBOFAN ENGINE

By
T. R. Clements

PRATT & WHITNEY AIRCRAFT
FLORIDA RESEARCH AND DEVELOPMENT CENTER
BOX 2691, WEST PALM BEACH, FLORIDA 33402

Prepared For
NATIONAL AERONAUTICS AND SPACE ADMINISTRATION

6 AUGUST 1970

Contract NAS3-11159

NASA Lewis Research Center
Cleveland, Ohio

P. J. Perkins, NASA Project Manager
Air Breathing Engine Procurement Section

FOREWORD

This interim report was prepared by the Pratt & Whitney Aircraft Division of United Aircraft Corporation under Contract NAS3-11159.

The contract was administered by the Air-Breathing Engine Procurement Section of the National Aeronautics and Space Administration, Lewis Research Center, Cleveland, Ohio.

The report summarizes the technical effort that was conducted during the period June 1968 through March 1970.

ABSTRACT

A performance development program is being conducted on an advanced short length combustor for operation at flight speeds up to Mach 3.0. The combustor has an outer diameter of 40 inches (1.016 m) and a length of 12 inches (0.305 m). The overall diffuser-combustor length is 20 inches (0.508 m).

Performance data were obtained in a 90-degree (1.57-radian) sector rig at a pressure level of 16 psia (11.03 N/cm^2). Inlet temperature and Mach number simulated sea level take-off operation.

Various combustor and diffuser configurations were investigated to simplify design and to improve performance. At a combustor temperature rise of 1640°F (911°K) good outlet temperature pattern factor (TPF = 0.14), radial profile, and combustion efficiency (100%) were obtained. The combined diffuser-combustor total pressure loss was 5.6%.

TABLE OF CONTENTS

TABLE OF CONTENTS (Continued)

ILLUSTRATIONS

ILLUSTRATIONS (Continued)

ILLUSTRATIONS (Continued)

ILLUSTRATIONS (Continued)

90-DEGREE SECTOR DEVELOPMENT OF A SHORT LENGTH COMBUSTOR FOR A SUPERSONIC CRUISE TURBOFAN ENGINE INTERIM REPORT

BY T. R. CLEMENTS

PRATT & WHITNEY AIRCRAFT
FLORIDA RESEARCH AND DEVELOPMENT CENTER

SUMMARY

A performance development program is being conducted on a short length combustor for turbofan engines operating at flight speeds up to Mach 3.0. The combustor is a double annulus, ram-induction type, sized for a large augmented turbofan engine. The combustor has an outer casing diameter of 40 inches (1.016 m) and a length of 12 inches (0.305 m) from fuel nozzle to turbine inlet vane. The combined diffuser-combustor length is 20 inches (0.508 m).

Testing was conducted in a 90-degree (1.57-radian) sector rig operating at ambient pressure level. Inlet temperatures and Mach numbers simulated engine sea level take-off operation. Data were recorded at combustor outlet temperature levels as high as 2350°F (1560.9°K).

The combustor demonstrated excellent performance. The outlet temperature pattern factor and combustion efficiency were 0.14 and 100% respectively at a temperature rise of 1638°F (1166.5°K). The combined diffuser-combustor total pressure loss was 5.6% at the sea level take-off inlet Mach number of 0.244.

Various combustor and diffuser configurations were investigated to simplify design and to improve performance. These included seven combustor liner configurations, two diffuser types, and several developmental modifications. The liner configurations were designed to provide information on the performance effects of the following air entry scoop variables:

1. The number of air entry scoops was reduced from 512 scoops to 256 scoops to simplify the design and reduce fabrication costs.

2. The ratio of primary to secondary air entry scoop area was increased from a value of 0.75 to 1.00.

3. The ratio of the OD and ID scoop area to center scoop area was increased from a value of 1.50 to 2.50.

4. The secondary scoop air injection was changed from full radial to have a 45-degree (0.785-radian) circumferential component.

5. The secondary scoop air injection was changed from full radial to have a 45-degree (0.785-radian) upstream component.

6. The center liner scoops were relocated to change the relative scoop pattern from a staggered to an opposed pattern.

Of the above liner configurations, only the design with the reduced number of scoops showed improved performance over that of the initial design. The 256-scoop combustor gave the best performance in an improved diffuser.

The initial diffuser design had severe flow uniformity problems due to airflow separation from the diffuser struts. This was corrected by modifying the diffuser splitter vanes to eliminate diffusion downstream of the splitter inlet. A further improvement in flow uniformity was made by designing another diffuser with smaller diffusing angle and a snout-type flow spreader.

Concurrent with this test program, the NASA is conducting tests on a 360-degree (6.282-radian) annular combustor of similar design. Tests with that combustor at elevated inlet temperature and pressure (1150°F (894.3°K) and 90 psia (62.05 N/cm^2)) revealed that the firewall was overheating. A partial solution evaluated on the 90-degree (1.57-radian) sector was made by installing improved cooling deflectors around each nozzle location and increasing the airflow sweeping the firewall lip. These cooling improvements had no noticeable effects on combustor performance.

INTRODUCTION

The operation of aircraft, such as the proposed supersonic transport, at sustained flight speeds of Mach 3.0 and at altitudes in excess of 50,000 feet (15,250 m) places severe operating constraints on the propulsion system. The high temperatures, 1150°F (894.3°K) at the combustor inlet, experienced by engines operating at Mach 3.0 increases the difficulty of cooling the various engine components. The relatively low lift/drag ratio of supersonic aircraft requires that structures be as light as possible to achieve useful payloads. This results in a need for smaller, lighter engines.

These conditions of high inlet air temperature and low total weight applied to the combustion system generally result in an attempt to shorten the combustor. This eases the cooling problem as there is less surface area to cool, and allows reductions in engine weight to be realized. However, good performance in a short length combustor is difficult to achieve since the available distance for burning and mixing is reduced.

To achieve good performance in a short length combustor, the NASA Lewis Research Center and Pratt and Whitney Aircraft have been conducting a test program on a double-annular, ram-induction combustor (sometimes referred to as a twin-ram combustor). This combustor has a double annular

primary combustion zone and utilizes ram air scoops to turn the airflow into the combustor. An earlier program (NAS3-7095) demonstrated the potential of this combustor concept to achieve good performance in a total diffuser-combustor length of 20 inches (0.508 m) (reference 1).

The objective of the present program is to further develop this concept. The program consists of two major tasks:

1. To conduct testing with different liner and diffuser configurations to determine the effects of combustor geometry on performance, to improve performance, and to simplify design and reduce fabrication costs. The initial scoop configuration evaluated was based on the final design from the earlier program.

2. To provide sector rig tests in support of a concurrent program being conducted by the NASA Lewis Research Center on a 360-degree (6.282-radian) annular combustor of similar design. Good correlation of sector and full annular performance results permitted solving of problems in the sector rig.

The test program is being conducted at the Pratt & Whitney Aircraft Florida Research and Development Center in a sector rig which is a quarter section of a full annulus. All testing has been performed at ambient pressure levels.

SCOPE OF THE INVESTIGATION

The test program included the performance evaluation of seven liner air entry scoop configurations, two diffuser geometries, and two swirler configurations. In addition, the program aided in solving problems encountered in the NASA 360-degree (6.282-radian) annular combustor test program. A brief description of the test hardware is presented below. A more detailed description is presented in Appendix A.

The liner configurations tested were:

Model 1 - Liner air entry scoops designed from final results of previous development effort. These liners were used as a baseline for comparing the various scoop and diffuser designs.

Model 2 - Number of scoops in a 360-degree (6.282-radian) annular combustor was reduced from 512 to 256 to simplify fabrication and to reduce costs. The scoops were twice the size of the Model 1 liner scoops to maintain the same liner flow area. The scoops were arranged so that the scoop pattern repeated once per nozzle spacing instead of twice per nozzle spacing as in the Model 1 liners.

Model 3 - Primary to secondary air entry scoop area increased approximately 33% over the Model 1 liners.

Model 4 - OD and ID liner to center liner air entry scoop area increased approximately 67% over the Model 1 liners.

Model 5 - Secondary scoop discharge provided a 45-degree (0.785-radian) upstream flow component compared to full radial injection in the Model 1 liners.

Model 6 - Secondary scoop discharge provided a 45-degree (0.785-radian) circumferential flow component compared to full radial injection in the Model 1 liners.

Model 7 - Liners identical to the Model 1 except that the center liner was rotated so that corresponding scoops (primary and secondary) were opposed instead of staggered.

The diffuser configurations tested were:

1. A 14-degree (0.244-radian) equivalent conical angle (ECA), spreader-type diffuser (ECA is defined in Appendix D).

2. A 7-degree (0.122-radian) ECA snout type diffuser.

The swirler configurations tested were:

1. A radial inflow air swirler which directed air radially over the fuel nozzle face.

2. An axial flow air swirler which admitted air into the combustion zone in an axial direction.

Most performance tests were conducted at the following nominal test conditions:

Inlet total pressure	=	16 psia (11.03 N/cm^2)
Inlet total temperature	=	600°F (588.7°K)
Reference velocity	=	100 ft/sec (30.40 m/sec) (corresponds to an inlet Mach number of 0.244)
Outlet average temperature	=	2200°F (1477.6°K)

For most of the tests a flat inlet velocity profile was used. However, the sensitivity of the combustor to inlet airflow distortion was periodically checked using a profile typical of supersonic engine compressors.

The test rig was instrumented to measure the following:

1. Combustor airflow

2. Combustor fuel flow

3. Inlet total and static pressure

4. Inlet total temperature

5. Outlet total temperature

6. Outlet total pressure (outlet static pressure was assumed to be ambient)

Details of the complete test apparatus are given in Appendixes B and C.

COMBUSTOR DESIGN

Double-Annular, Ram-Induction Principle. - The combustor used in this investigation is referred to as a Double-Annular, Ram-Induction Combustor (sometimes called Twin-Ram Induction Combustor). The term ram-induction arises because the air enters the combustor by the ram pressure of the inlet airflow. The airflow is efficiently turned into the combustion zone by several rows of vaned turning elbows or scoops, figure 1. This is contrasted with more conventional combustion systems where the airflow is first diffused to very low Mach numbers to increase the stream static pressure. The air is then forced to enter the combustor by the static pressure differential across the chamber walls.

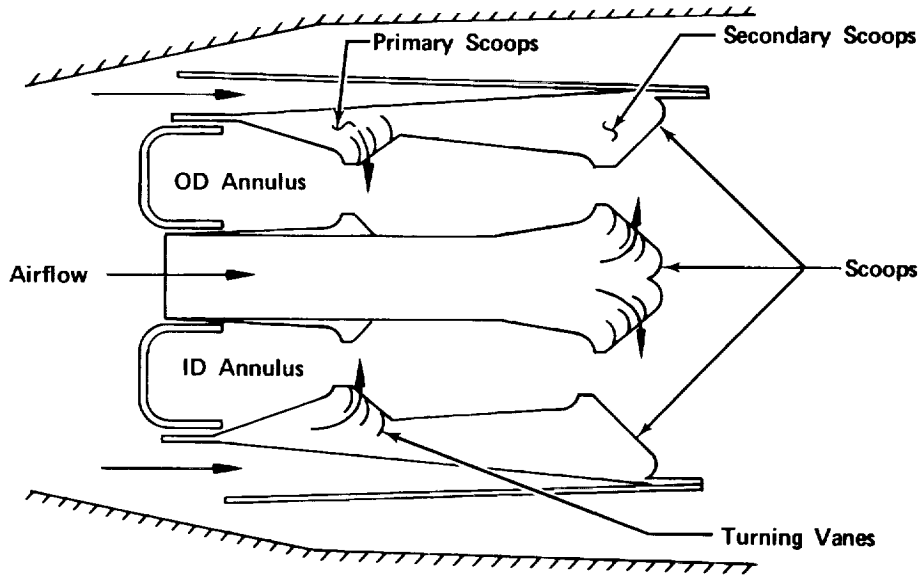

Figure 1. Ram Induction Concept in a Double-Annular Combustor

Ram induction offers several advantages over conventional static pressure fed systems:

1. Better control of the airflow injection angle is obtained with the vaned turning scoops. This allows a shorter length combustor because more intense mixing can be established in the combustion zone.

2. Diffuser length can be shortened since diffusion to very low Mach numbers is no longer needed or desired. The overall diffuser-combustor length can therefore be reduced. The short length, small area ratio diffuser could have less pressure loss since it is not as prone to flow separation. However, this may be offset due to increased turning losses associated with spreading the relatively high velocity flow evenly around the combustor.

3. The uniformity of the airflow supplied to the combustor is improved since a small area ratio diffuser with conservative equivalent conical angles (ECA) virtually eliminates diffuser stall.

4. The high velocity flow over the exterior surfaces of the combustor provides substantial convective cooling of these walls. This reduces the film cooling air requirement making more air available for mixing and temperature profile tailoring.

A more detailed discussion of the ram-induction concept is provided in reference 2.

Constructing the combustion zone as a double-annulus allows reducing the combustor length while maintaining an adequate ratio of effective combustor length to annulus height. This feature allows considerable reductions in combustor length to be made over that provided by use of the ram-induction concept alone. For example, figures 2a and 2b show a comparison of a single annulus, ram-induction combustor, tested by P&WA and the NASA (reference 3), with the double-annular, ram-induction combustor. These combustor systems were designed to operate at similar conditions of Mach number, airflow, temperature, and pressure. The figures show that the combined diffuser-combustor length of the double-annular, ram-induction combustor is 10 inches (0.254 m) shorter. The double-annular combustor installed in the 14-degree (0.244-radian) ECA diffuser and the 7-degree (0.122-radian) ECA snouted diffuser is shown in figures 3a and 3b.

Individual control of the inner and outer annulus fuel systems of the double-annular combustion zone provides a powerful method for tailoring the outlet radial temperature profile.

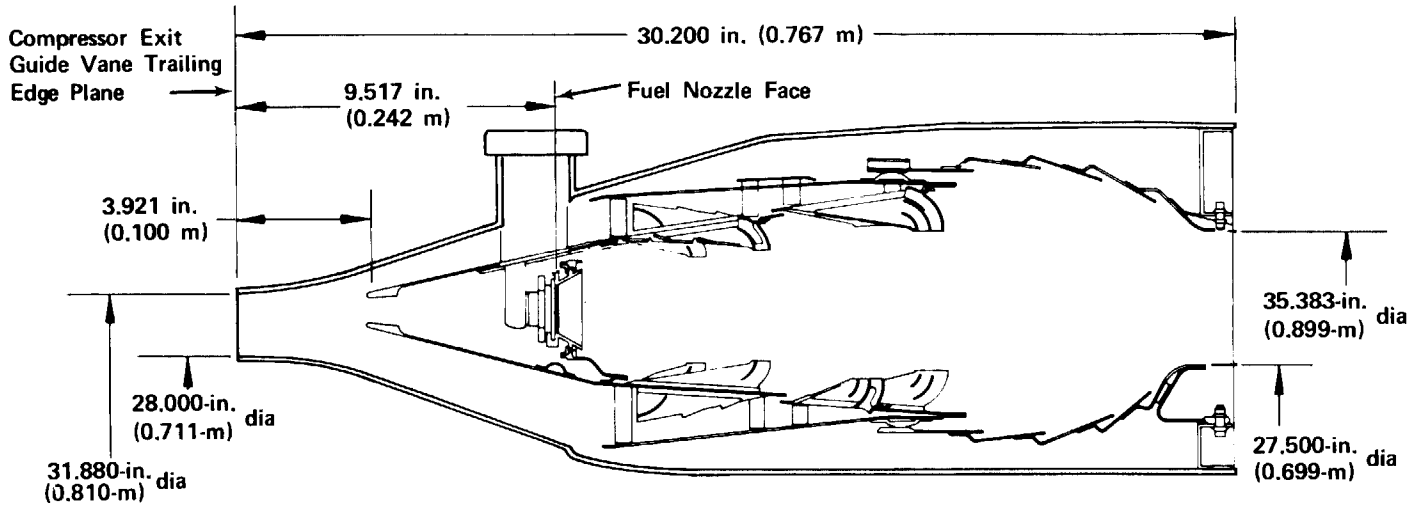

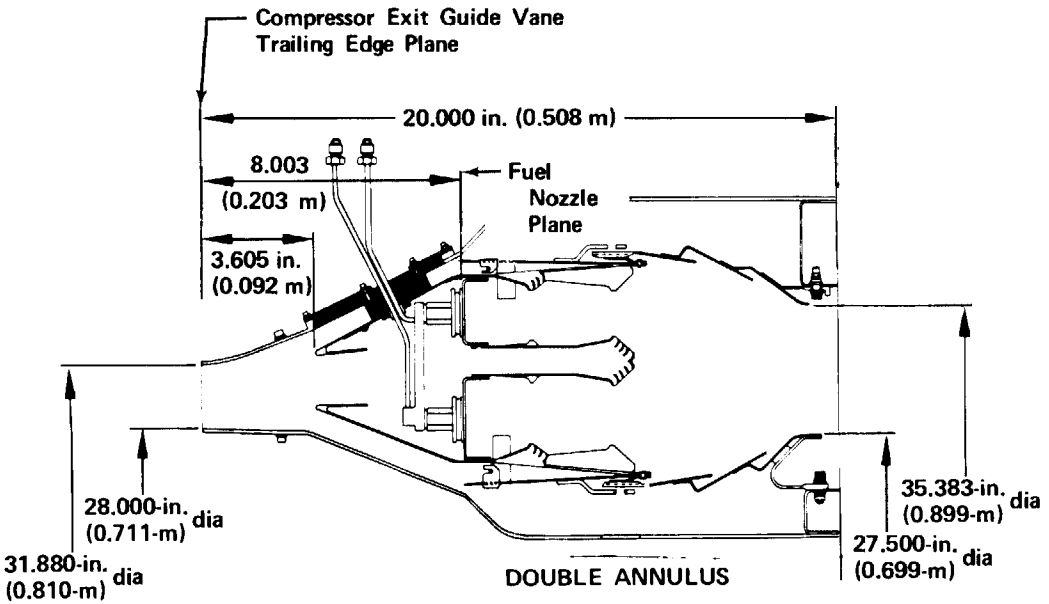

Figure 2a. Single- and Double-Annulus, Ram-Induction Combustors

FD 36584

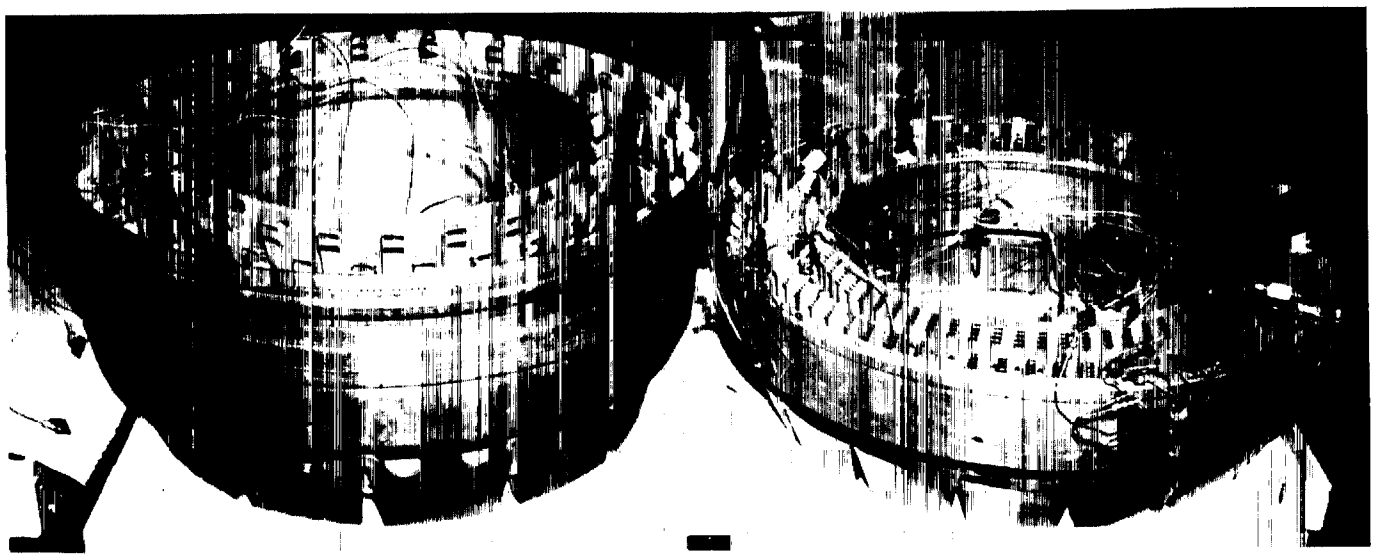

Figure 2b. Double-Annular Short-Length Combustor Compared to Single-Annular Combustor for Same Operating Requirements (Exit Transition Liners Removed)

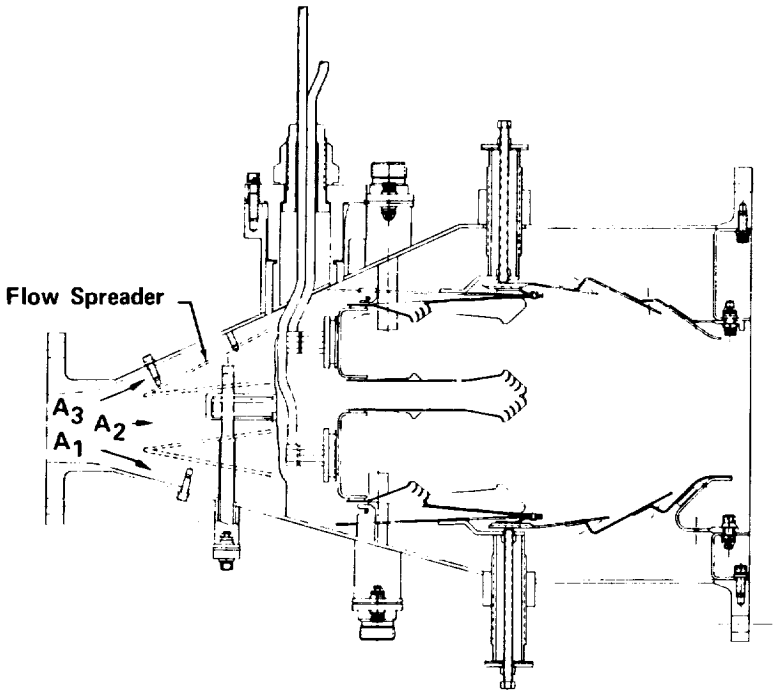

Figure 3a. Double-Annular, Ram-Induction Combustor Installed in 14-Degree ECA, Flow Spreader Diffuser

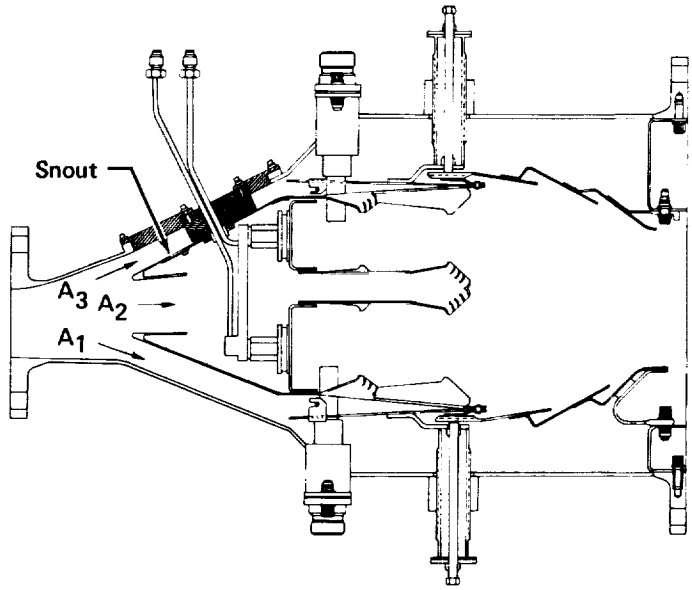

Figure 3b. Double-Annular, Ram-Induction Combustor Installed in 7-Degree ECA, Snouted Diffuser

CALCULATIONS

Performance calculations included the determination of inlet Mach number, reference velocity, combustion efficiency, total pressure loss, and the outlet temperature uniformity parameters, TPF and δrotor.

Inlet Mach Number. - Calculated from continuity using the average inlet static pressure and assuming one-dimensional isentropic flow. Therefore:

$$M_{n3} = \frac{W_{a3}\sqrt{T_{t3}}}{P_{s3}\,A_3}\sqrt{\frac{R}{\gamma\left[1+\left(\frac{\gamma-1}{2}\right)M_{n3}^{2}\right]}} \qquad \text{(Eq 1)}$$

where:

M_n = Mach number

W_a = Airflow

T_t = Average total temperature of 3 readings

P_s = Average static pressure of 5 readings

A = Area

γ = Ratio of specific heats

R = Gas constant

The subscript 3 refers to the diffuser inlet plane.

Combustor Reference Velocity. - Calculated assuming constant density flow from the diffuser inlet to the reference area. The reference area is defined as the inlet area between the inner and outer shrouds (approximately 662.76 in^2 (0.428 m^2)). The calculation considers only that portion of the airflow, based on combustor area splits, passing through the shrouds; transition duct airflow is not figured in the calculation. Therefore:

$$V_{ref} = \frac{W_{a3} - W_{t/d}}{\rho_3\,A_s} \qquad \text{(Eq 2)}$$

where:

$W_{t/d}$ = Transition duct airflow

A_s = Shroud area

ρ_3 = Air density at diffuser inlet

Combustion Efficiency. - Defined as the ratio of the measured temperature rise to a theoretical temperature rise. The theoretical rise is calculated from the fuel-air ratio, fuel properties, inlet temperature, and the amount of water vapor present in the inlet airflow. The efficiency is expressed as:

$$Eff_{mb} = \frac{T_{t4m} - T_{t3}}{T_{t4w} - T_{t3}} \qquad \text{(Eq 3)}$$

where:

T_{t4m} = Mass weighted average of 105 outlet total temperatures (The procedure used for calculating the mass weighted average is presented in Appendix E.)

T_{t4w} = Theoretical outlet total temperature (The procedure used in calculating the ideal outlet temperature with humid air is given in Appendix E.)

Total Pressure Loss. - The combined diffuser-combustor total pressure loss is given by:

$$\frac{\Delta P}{P} = \frac{P_{t4} - P_{t3}}{P_{t3}} \qquad \text{(Eq 4)}$$

where:

P_{t3} = Mass weighted average of 25 inlet total pressures

P_{t4} = Mass weighted average of 105 outlet total pressures

and is expressed as a percentage value.

Outlet Temperature Pattern Factor (TPF). - Defined as the ratio of the maximum positive deviation from the average outlet temperature to the average temperature rise, or:

$$TPF = \frac{T_{t4\ max} - T_{t4}}{T_{t4} - T_{t3}} \qquad \text{(Eq 5)}$$

where:

$T_{t4\ max}$ = Maximum temperature at any location in the combustor outlet.

Outlet Radial Temperature Profile. - Determined from the average of 21 outlet total temperatures measured circumferentially at each of 5 radial positions.

δrotor. - Defined as the ratio of the maximum positive deviation of the measured outlet radial temperature profile from a desired radial temperature profile to the desired temperature rise, or:

$$\delta\text{rotor} = \frac{\left[T_{t4j} - T_{t4j\ \text{desired}}\right]_{\max}}{T_{t4\ \text{desired}} - T_{t3}} \qquad \text{(Eq 6)}$$

The "j" subscript refers to any radial location in the radial temperature profile. Note that the deviation is the maximum positive deviation at any radial location. Figure 4 is a graphical explanation of δrotor. Since the desired profile is defined for some given outlet average temperature (in this case 2200°F (1477.6°K)) the measured profile must be normalized to that average temperature before comparison is made. This correction procedure is presented in Appendix E.

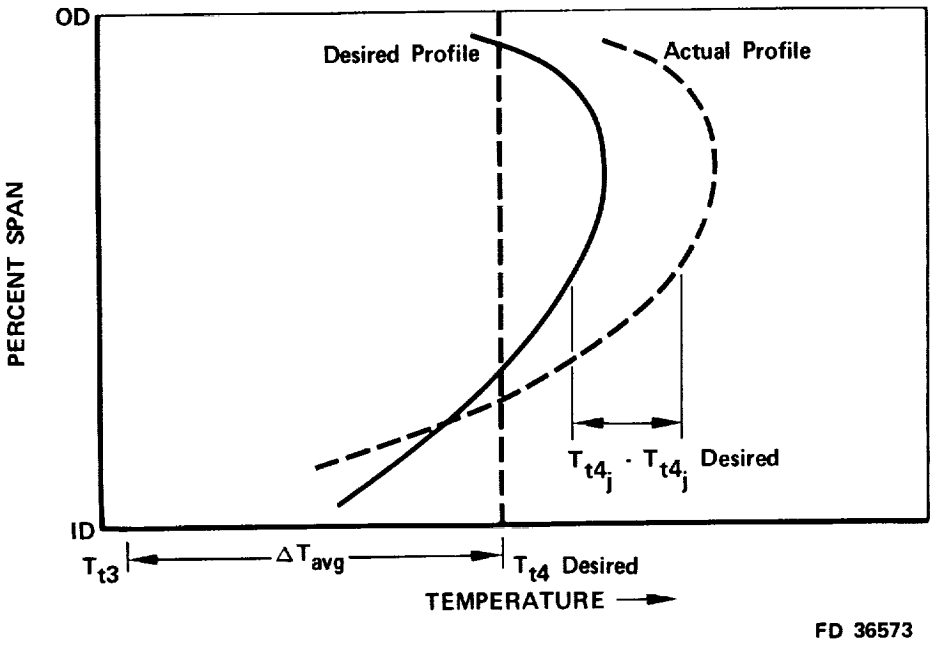

Figure 4. Explanation of Terms in δrotor Expression

RESULTS AND DISCUSSION

Diffuser-Combustor Configuration With Best Performance. - The diffuser-combustor combination which gave the best overall performance was the Model 2, 256-scoop combustor (1/2 the number of scoops in the Model 1 combustor) installed in the 7-degree (0.122-radian) ECA, snouted diffuser. Figure 5a shows the assembled combustor. Comparison with the Model 1 initial design combustor (figure 5b) shows the Model 2 combustor to be less complex. Table 1 compares the performance of this combustor with the other configurations tested. The outlet temperature pattern factor was the lowest obtained (TPF = 0.14). Combustion efficiency was 100%. The combined diffuser-combustor total pressure loss was 5.6% at an inlet Mach number of 0.244. This pressure loss is comparable with any of the other configurations tested.

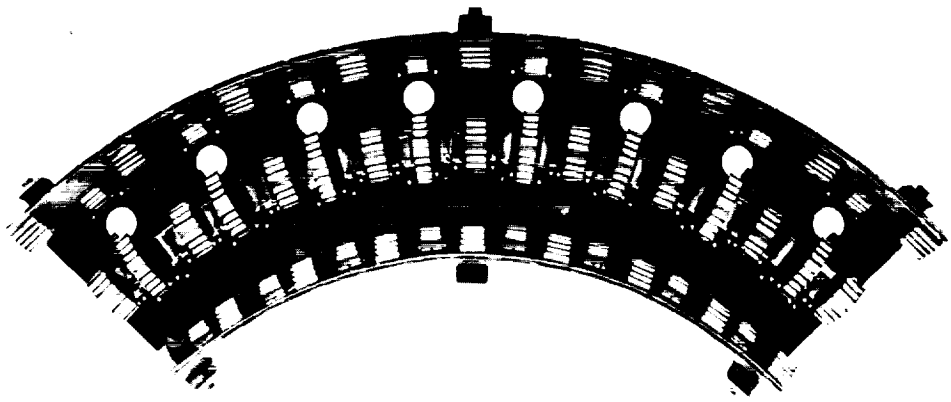

FE 89706
FD 36594

Figure 5a. Model 2, 256-Scoop Combustor (Number of Scoops for a Full Annulus)

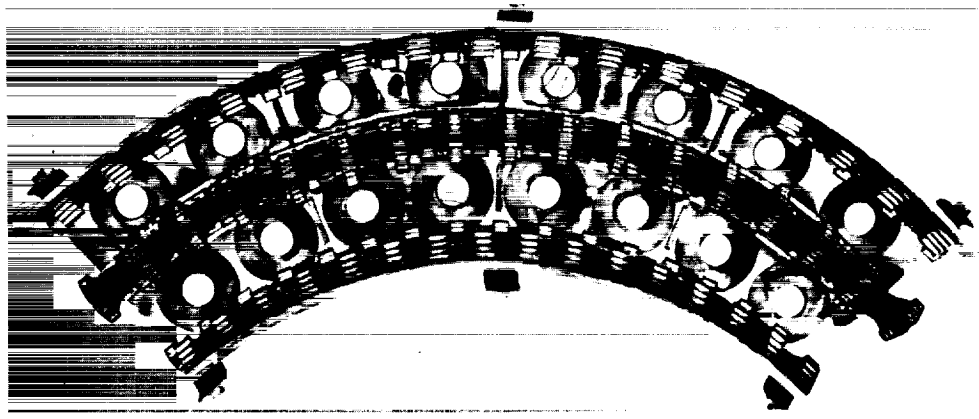

FE 91396
FD 36592

Figure 5b. Model 1, 512-Scoop Combustor (Number of Scoops for a Full Annulus)

Table 1. Summary of Co

Model No.	Description: Scoops	Description: Diffuser	Test Conditi
1	Initial design baseline scoops. Assembled combustor had 512 scoops in a 360-degree annular combustor. The primary to secondary area ratio was 0.75 and the OD and ID to center scoop area ratio was 1.50.	14-degree (0.244-radian) ECA, flow spreader diffuser	T_{t3} = 599°F (5 M_{n3} = 0.256 Flat inlet vel profile
		7-degree (0.122-radian) ECA, snout type diffuser	T_{t3} = 601°F (5 M_{n3} = 0.244 Flat inlet vel profile
2	Reduced number of scoops. Design had 256 scoops in a 360-degree annular combustor. The primary to secondary area ratio was 0.75 and the OD and ID to center scoop area ratio was 1.50.	7-degree (0.122-radian) ECA, snout-type diffuser	T_{t3} - 600°F (5 M_{n3} = 0.245 Flat inlet vel profile
			T_{t3} = 600°F (5 M_{n3} = 0.242 Distorted inle velocity profi
			T_{t3} = 597°F (5 M_{n3} = 0.242 Flat inlet vel profile
3	Primary to secondary area ratio increased from 0.75 to 1.00.	7-degree (0.122-radian) ECA, snout-type diffuser	T_{t3} = 607°F (5 M_{n3} = 0.246 Flat inlet vel profile
4	Ratio of OD and ID liner scoop area to center liner scoop area increased from 1.50 to 2.50.	14-degree (0.244-radian) ECA, flow spreader diffuser	T_{t3} = 596°F (5 M_{n3} = 0.245 Flat inlet vel profile
5	Upstream flow of secondary air entry scoops.	14-degree (0.244-radian) ECA, flow spreader diffuser	T_{t3} = 589°F (5 M_{n3} = 0.249 Flat inlet vel profile
6	Tangential flow of secondary air entry scoops.	7-degree (0.122-radian) ECA, snout-type diffuser	T_{t3} = 597°F (5 M_{n3} = 0.245 Flat inlet vel profile
7	Model 1 liners with center liner rotated so that corresponding scoop (primary and secondary) were opposed.	14-degree (0.244-radian) ECA, flow spreader diffuser	T_{t3} = 596°F (5 M_{n3} = 0.248 Flat inlet vel profile

T_{t3} = Inlet average total temperature
M_{n3} = Inlet mach number
ΔT = Temperature rise across the combustor
N.A. = Not applicable

δrotor = Maxim desir
$\Delta P/P$ = Total
TPF = Ratio avera

mbustor Performance

on	Fuel Split OD/ID	Pattern Factor TPF	ΔT °F (°K)	Outlet Temp °F (°K)	ΔP/P at M_{n3} = 0.244	Efficiency	δrotor and Location
88 °K) ocity	1.00	0.21	1590 (1139)	2191 (1473)	5.0%	97%	0.059 50% span
89 °K) ocity	1.20	0.18	1533 (1107)	2184 (1441)	5.3%	101%	0.055 50% span
89 °K) ocity	1.13	0.14	1638 (999)	2238 (1499)	5.6%	100%	0.022 50% span
89 °K) t le	1.13	0.15	1699 (1199)	2299 (1533)	6.1%	104%	0.022 50% span
87 °K) ocity	1.07	0.16	1750 (1228)	2350 (1533)	5.7%	101%	N.A.
93 °K) ocity	1.10	0.26	1501 (1089)	2108 (1426)	5.5%	101%	0.033 70% span
86 °K) ocity	1.04	0.30	1506 (1092)	2102 (1423)	5.9%	100%	0.029 50% span
83 °K) ocity	1.0	0.30	1528 (1104)	2117 (1431)	5.9%	97%	0.048 50% span
87 °K) ocity	1.10	0.37	1456 (1064)	2053 (1396)	5.9%	101%	N.A.
86 °K) ocity	1.14	0.29	1552 (1117)	2148 (1449)	5.1%	103%	0.043 70% span

um deviation of measured profile from a desired profile ratioed to the
ed temperature rise
pressure loss as a percent of inlet total pressure
of the maximum outlet temperature deviation from the average to the
ge temperature rise

This combustor was tested with flat and distorted inlet velocity head profiles (figure 6) and at temperature rises up to 1750°F (1227.6°K). Table 1 shows that the combustor pattern factor and efficiency remained essentially unchanged in tests with the flat and distorted inlet velocity profiles. However, the system total pressure loss increased when the inlet airflow was distorted (6.1% as compared to 5.6%).

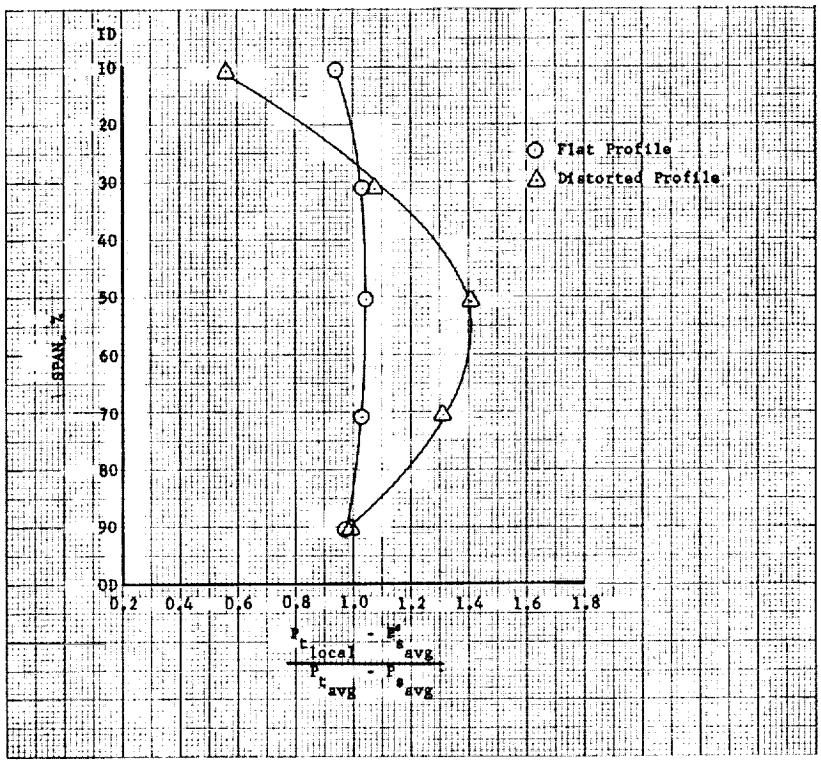

DF 79978

Figure 6. Typical Diffuser Inlet Velocity Head Profiles

The degree of inlet airflow distortion investigated had very little effect on the shape of the outlet radial temperature profiles. Figure 7 compares the temperature profiles obtained while operating with and without distorted inlet airflow. The desired temperature profile, considered typical of that required for high inlet temperature turbines, is included for comparison. The only difference is that the portion of the profile toward the combustor outer diameter is slightly hotter and the inner diameter portion slightly cooler with the distorted inlet. The value of δrotor, which expresses the maximum positive deviation of the profile from the desired profile, is the same both in magnitude and location (0.022 at midspan).

The nominal combustor temperature rise was 1600°F (888.9°K), however operating the combustor at a temperature rise of 1750°F (972°K) had no appreciable effect on combustor performance. The maximum temperature rise achieved was limited by durability requirements of the traverse probe rather than any degradation in combustor performance. Figure 8 shows that the outlet radial temperature profile remained unaffected over the range of temperature rises investigated.

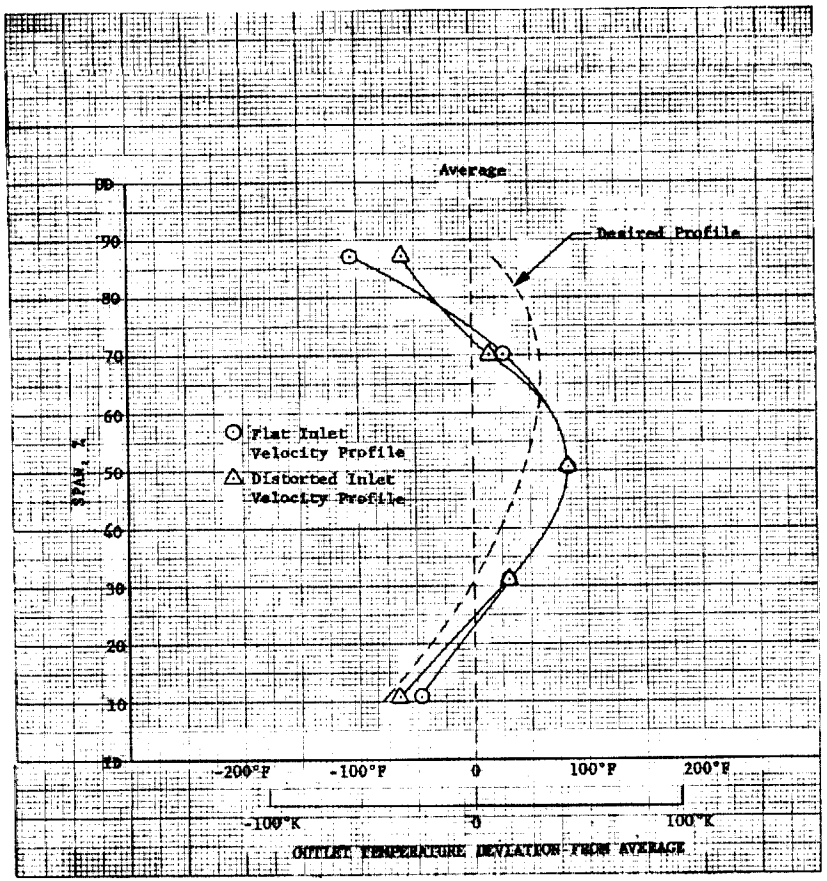

DF 79979

Figure 7. Comparison of the Outlet Radial Temperature Profiles With and Without Inlet Airflow Distortion, Model 2 Combustor

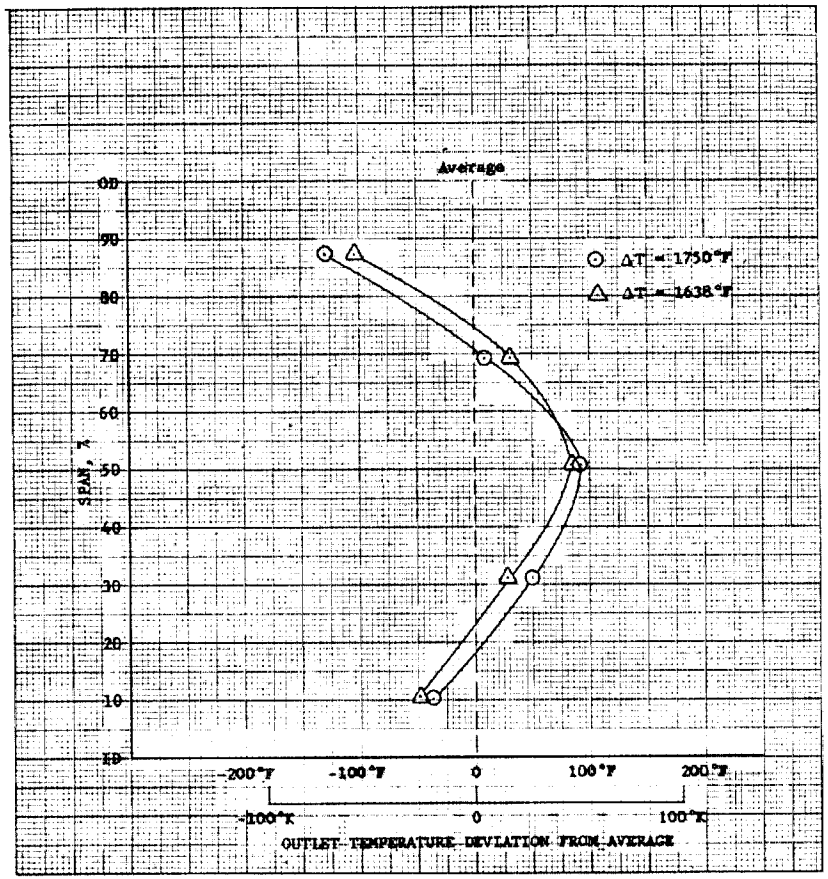

DF 79980

Figure 8. Comparison of the Outlet Radial Temperature Profiles at Temperature Rises of 1638°F and 1750°F, Model 2 Combustor

Figure 9 shows a typical outlet temperature distribution[1] for the Model 2 combustor. Little variation was observed in the distribution as a result of airflow distortion or increased temperature rise. Figure 9 does reveal one significant test result; the outer and the inner liner secondary scoop pattern is discernable in the temperature distribution. This suggests that the turbulent mixing forces in the combustor are not sufficient to eliminate individual scoop patterns. This could limit any future attempts to reduce the overall diffuser-combustor total pressure loss without seriously affecting the otherwise good performance of this combustor.

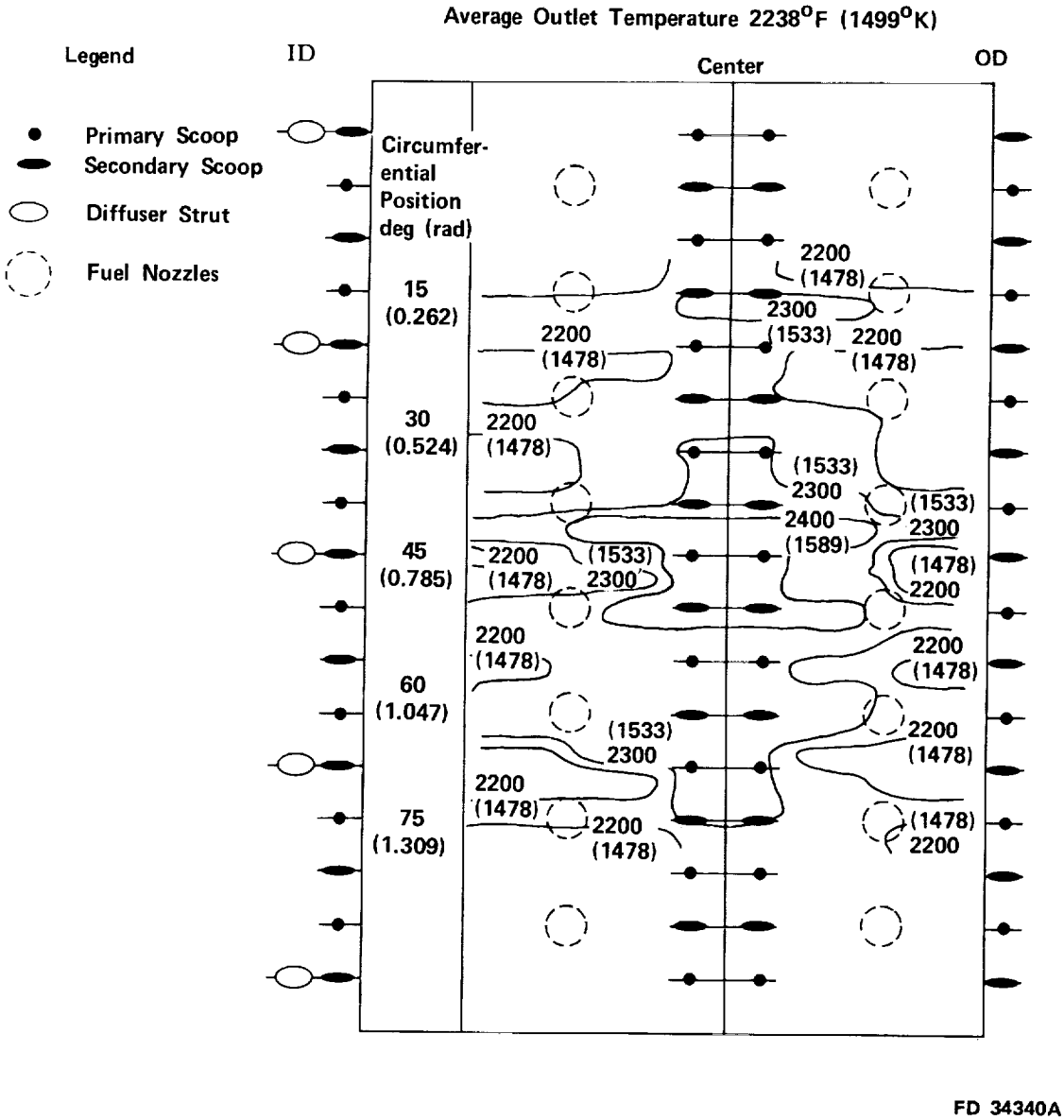

Figure 9. Outlet Temperature Distribution, Model 2 Combustor

[1] Outlet temperature distributions are shown in rectangular rather than true arc format to facilitate construction of the isotherms, which are drawn directly over the rectangular computer data printout.

Performance Effects of Liner Air Entry Scoop Variables. - In addition to the Model 2, 256-scoop combustor, other configurations were tested to study the effect of the following scoop variations on combustor performance:

1. Increasing the primary to secondary scoop area from a value of 0.75 to 1.00.

2. Increasing the ratio of the outside and inside diameter scoop area to center scoop area from a value of 1.50 to 2.50.

3. Changing the secondary scoop air injection from full radial to have a 45-degree (0.785-radian) circumferential component.

4. Changing the secondary scoop air injection from full radial to have a 45-degree (0.785-radian) upstream component.

5. Changing the relative scoop pattern from staggered to opposed.

Model 1 Initial Design Combustor Performance. - The Model 1 combustor was used for comparing the various configurations. This combustor, shown in figure 5b, had a primary to secondary area split of approximately 0.75. The ratio of the outer and inner liner scoop area to center liner scoop area was 1.50.

The performance of these liners in both the 14-degree (0.244-radian) ECA spreader-type and the 7-degree (0.122-radian) ECA snout-type diffusers was good (table 1, Model 1). The best temperature pattern factor (TPF) for the Model 1 combustor in the 7-degree (0.122-radian) ECA diffuser was 0.18. In the 14-degree (0.244-radian) ECA diffuser the best TPF was 0.21. The combustion efficiency with the combustor installed in the 14-degree (0.244-radian) ECA diffuser was 97%. In the 7-degree (0.122-radian) ECA diffuser the efficiency was 101%. The combined diffuser-combustor total pressure loss was the same, within experimental error, for both configurations (approximately 5.2%). Figure 10a compares the outlet radial temperature profiles obtained with the Model 1 combustor while operating in the 7-degree (0.122-radian) and 14-degree (0.244-radian) ECA diffusers. The profile shown for the 14-degree (0.244-radian) ECA diffuser was obtained by using a combustor outer-to-inner annulus fuel flow ratio of 1.0. The fuel flow ratio used with the 7-degree (0.122-radian) ECA diffuser was 1.2. Comparison of these different fuel flow ratios for the Model 1 combustor and 7-degree (0.122-radian) ECA diffuser combination is given in figure 10b. This demonstrates the effectiveness of the dual-annular fuel system in controlling the shape of the radial temperature profile.

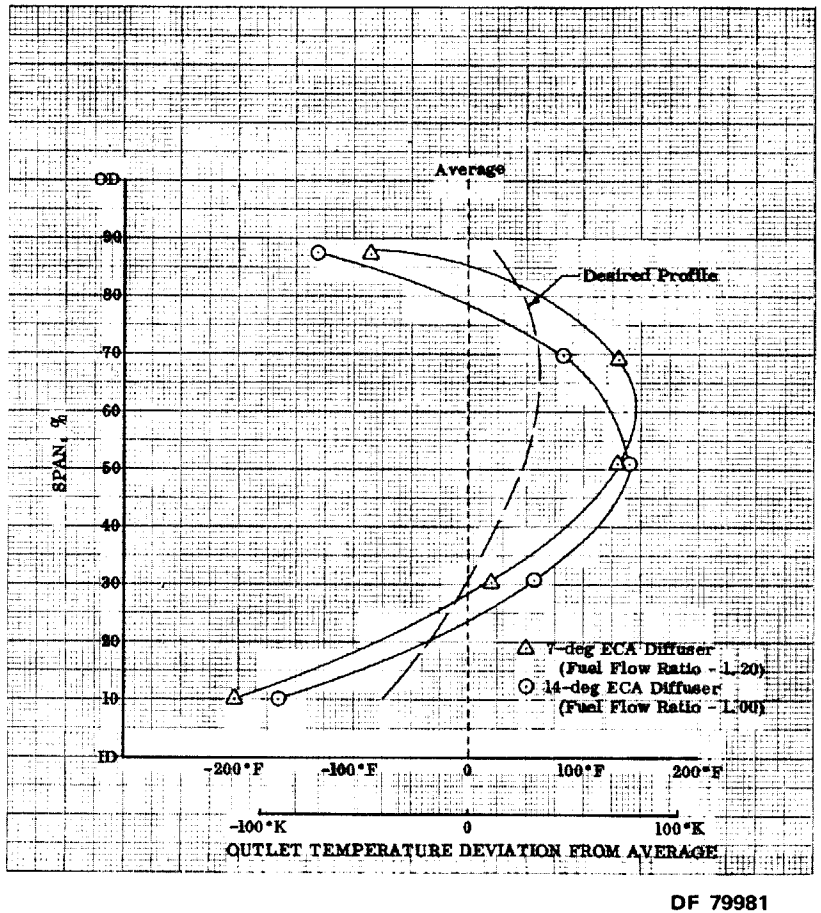

Figure 10a. Outlet Radial Temperature Profiles, Model 1 Combustor

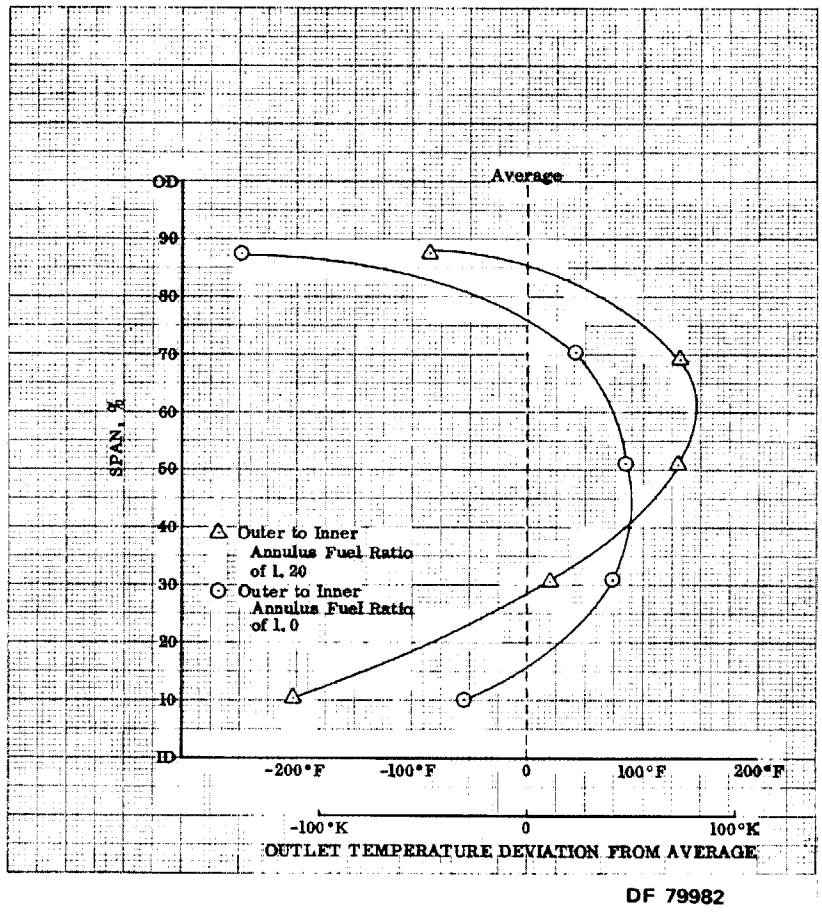

Figure 10b. Effect of Outer to Inner Annulus Fuel Flow Split on Outlet Radial Temperature Profile, Model 1 Combustor in 7-degree (0.122-radian) Diffuser.

Model 3 Increased Primary to Secondary Air Entry Scoop Area Liners. - These liners had their scoop discharge areas altered to increase the primary to secondary area ratio from 0.75 to 1.0. The total liner flow area was unchanged. The liners were tested in the 7-degree (0.122-radian) ECA, snouted diffuser so the Model 1 liners in this diffuser were used for comparison.

Figure 11 shows that the combustor TPF increased from 0.18 to approximately 0.24 with the increase in primary to secondary area split. The combined diffuser-combustor total pressure loss increased slightly from 5.2% to approximately 5.5% (figure 12). Combustor efficiency was unchanged (101%, table 1, Model 3).

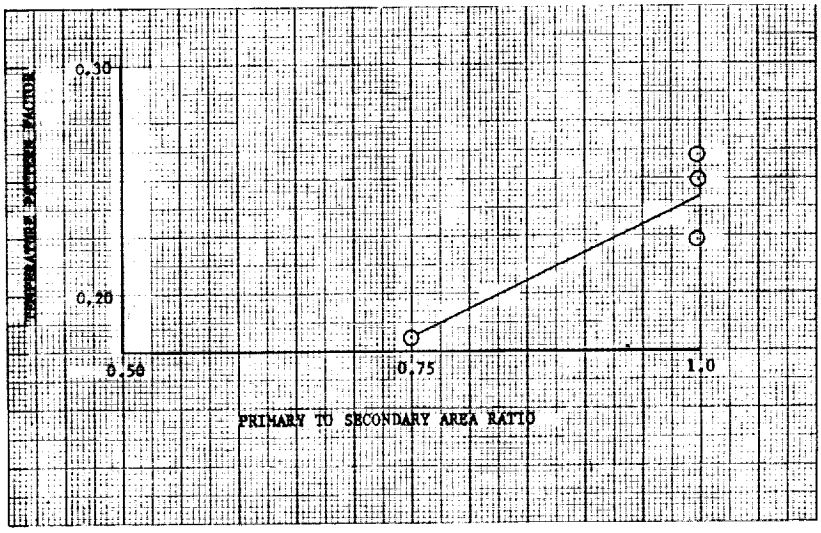

Figure 11. Temperature Pattern Factor vs P/S Ratio

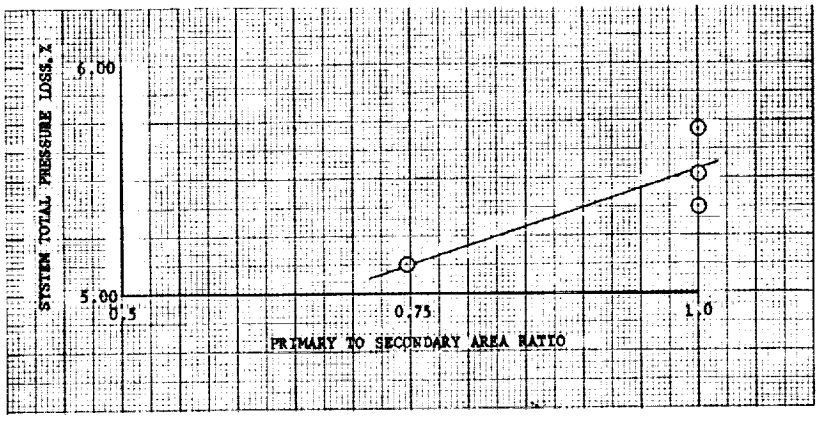

Figure 12. Combined Diffuser-Combustor $\Delta P/P$ vs P/S Ratio

The outlet radial temperature profile, figure 13, is a better approximation of the desired profile than that of the Model 1 liners. The value of δrotor was 0.033 at 70% span as compared to 0.059 at 50% span for the Model 1.

Model 4 Increased Ratio of OD and ID Liner Scoop Area to Center Liner Scoop Area. - These liners had their scoop discharge areas altered to increase the ratio of the outer and inner liner scoop area to center liner scoop area from 1.50 to 2.50. The total liner flow area was unchanged from the Model 1 liners. The liners were installed in the 14-degree (0.244-radian) ECA diffuser so the Model 1 liners in this diffuser were used for comparison.

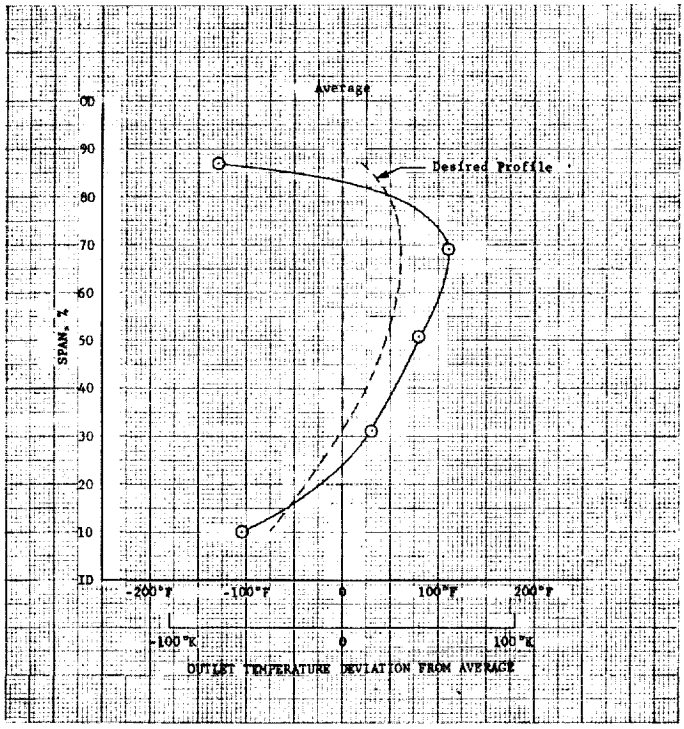

DF 79985

Figure 13. Outlet Radial Temperature Profile, Model 3 Combustor

The temperature pattern factor increased from 0.21 to 0.29 (figure 14). The combined diffuser-combustor total pressure loss increased from 5.0% to 5.9% (figure 15). Combustion efficiency improved to 100% compared to 97% for the Model 1 liners. Figure 16 shows the outlet radial temperature profile obtained with this combustor. The outer-to-inner annulus fuel flow ratio was 1.04. The profile closely resembles the profile obtained with the 256-scoop, Model 2 combustor (figure 7). In fact, except for the Model 2 combustor, δrotor was the best obtained in the program (0.029 at midspan).

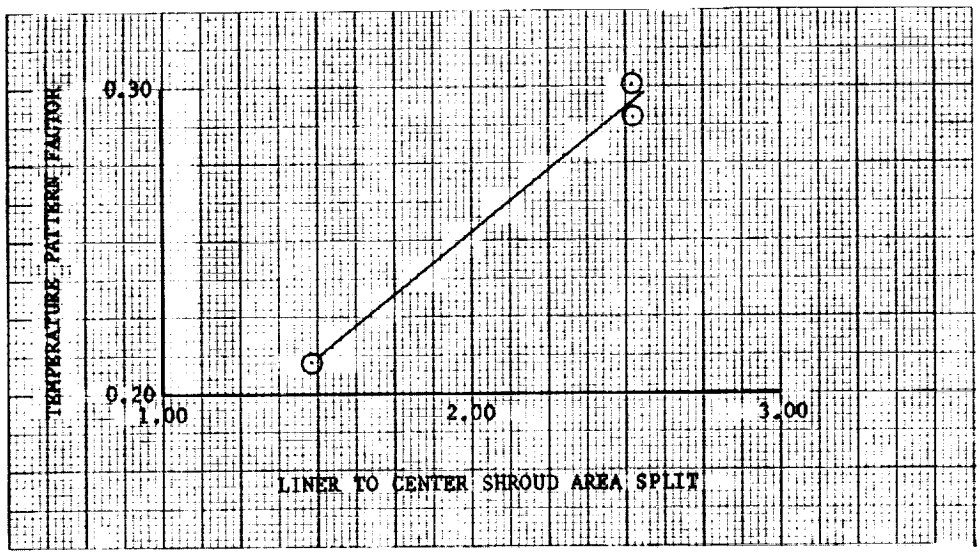

Figure 14. Temperature Pattern Factor vs OD and ID Liner to Center Liner Area Ratio, Model 4 Combustor

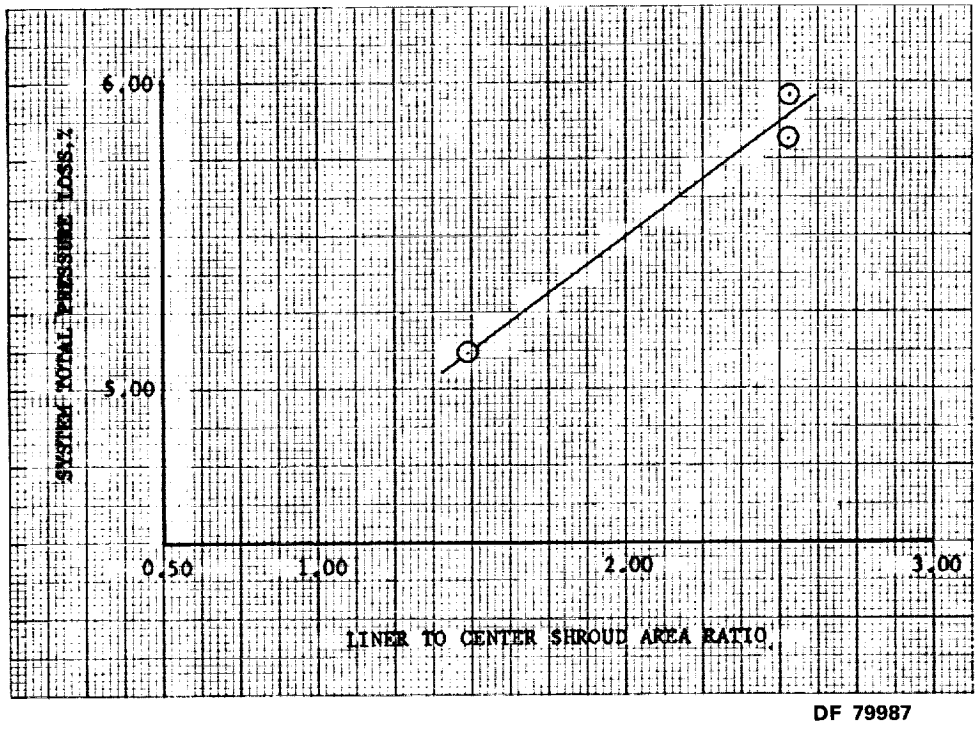

Figure 15. Combined Diffuser-Combustor $\Delta P/P$ vs OD and ID Liner to Center Liner Area Ratio, Model 4 Combustor

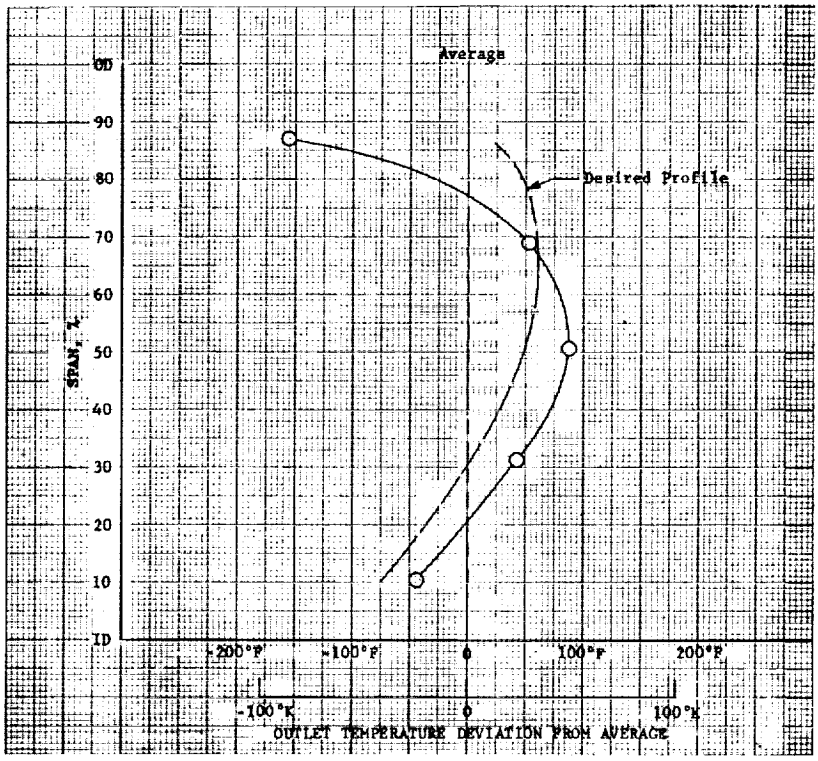

DF 79988

Figure 16. Outlet Radial Temperature Profile, Model 4 Combustor

Model 5 Upstream Flow Secondary Air Entry Scoop Liners. - These liners had secondary scoops designed to discharge the airflow with a 45-degree (0.785-radian) upstream flow component. Liner flow area and area splits were unchanged from the Model 1 combustor. The assembled combustor is shown in figure 17.

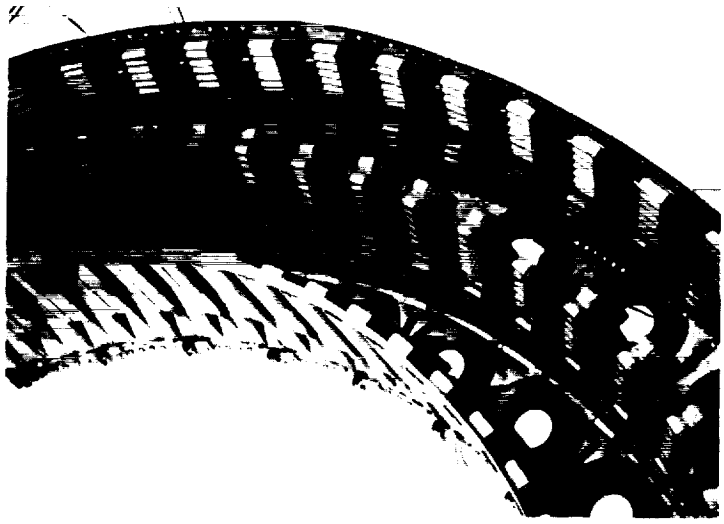

FE 96874
FD 36593

Figure 17. Model 5 Combustor

As expected, turning the secondary flow upstream increased the total pressure loss. The increase was from 5.0% for the Model 1 to 5.9%. The outlet temperature uniformity was also impaired as evidenced by the increase in the pattern factor from 0.21 to 0.29. The outlet radial temperature profile, figure 18, is a fair approximation of the desired profile. The value of δ_{rotor} was 0.048.

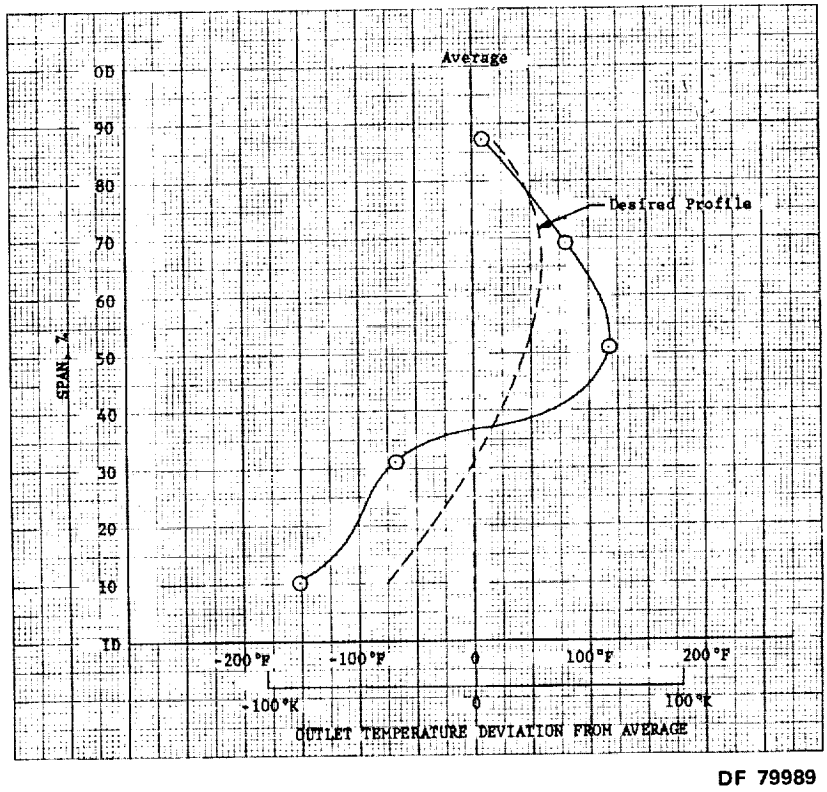

Figure 18. Outlet Radial Temperature Profile, Model 5 Combustor

Model 6 Tangential Flow of Secondary Air Entry Liners. - These liners featured secondary scoops having a 45-degree (0.785-radian) flow component in the circumferential direction. Liner flow area and area splits were unchanged from the Model 1 combustor. The assembled combustor is shown in figure 19. The opposed flow secondary scoop arrangement shown in figure 19 was the only configuration which could be tested in the sector rig. The configuration in which the secondary scoops discharge in the same direction might offer improved temperature pattern uniformity due to the swirling flow, but would be unduly influenced by the sector end walls.

The performance of this combustor was quite poor when compared to the Model 1 combustor. The temperature pattern factor was 0.37 as compared to 0.18 for the Model 1 liners (table 1, Model 6). Approximately 60% of the measured pattern factor was due to the extreme center peakedness of the outlet radial temperature profile shown in figure 20. The overall total pressure loss was 5.9% compared to 5.3% for Model 1.

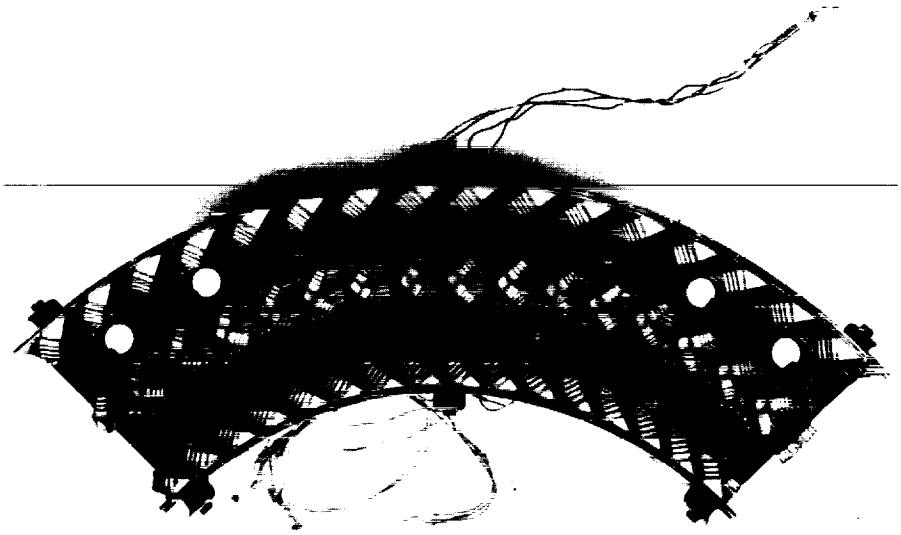

FE 89667
FD 36606

Figure 19. Model 6 Circumferential Air Directed Secondary Scoop Combustor

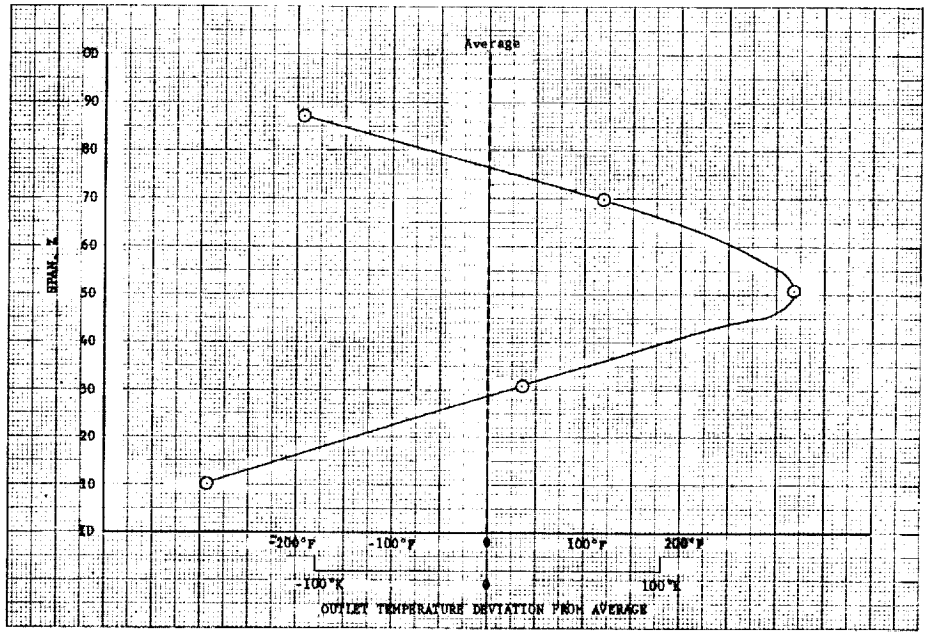

DF 79990

Figure 20. Outlet Radial Temperature Profile, Model 6 Combustor

Model 7 Opposed Scoops. - All of the above combustors featured scoop patterns that had scoops on the center liner circumferentially staggered in relation to their corresponding scoops on the outer and inner liners. This configuration used the Model 1 liners with the center liner indexed so that corresponding scoops on all liners were opposed (see figure 21).

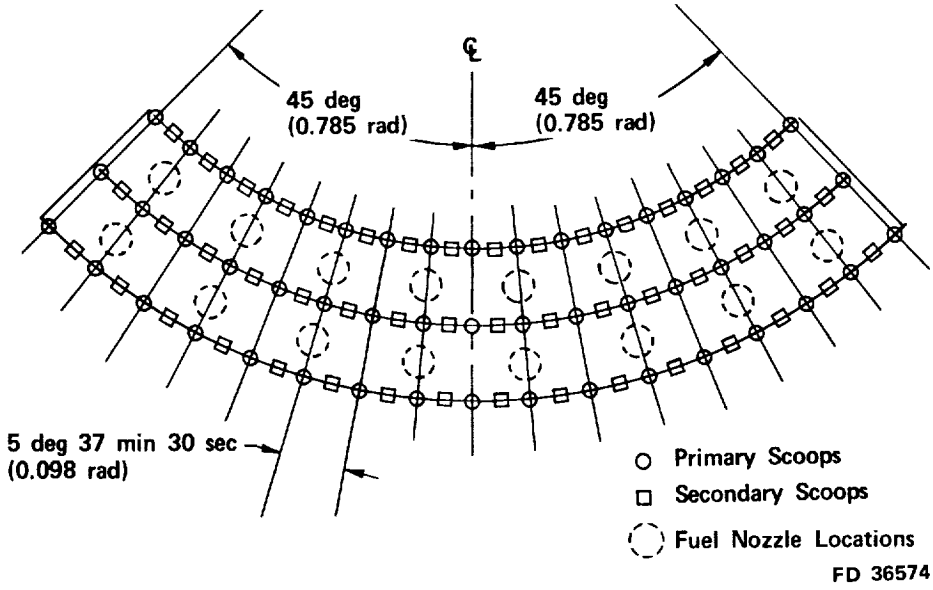

Figure 21. Opposed Scoop Pattern, Model 7 Combustor

The opposed scoop arrangement impaired the uniformity of the outlet temperature pattern. The pattern factor increased from 0.21 to 0.29 (table 1, Model 7). This scoop geometry caused a reduction in the turbulent mixing as indicated by the reduced midspan temperature in the radial temperature profile (figure 22). The combustion efficiency (103%) and total pressure loss (5.1%) were unaffected by the opposed scoop pattern.

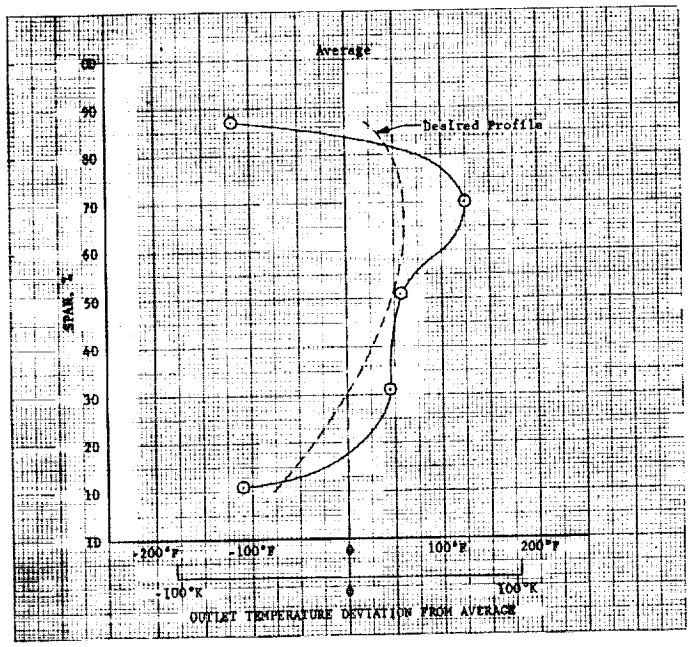

Figure 22. Outlet Radial Temperature Profile, Model 7 Combustor

Performance Effects of Diffuser Configurations. - The Model 1 combustor was tested in the 7-degree (0.122-radian) ECA, snout-type diffuser (figure 23a) and the 14-degree (0.244-radian) ECA, spreader-type diffuser (figure 23b). These tests allowed a performance comparison of these diffusers to be made. The performance criteria of interest were diffuser total pressure loss and airflow uniformity as affecting the outlet temperature profile.

The overall diffuser-combustor system total pressure loss for each configuration was the same within the limits of experimental error (table 1). Therefore, the total pressure loss of the diffusers was the same assuming a constant combustor pressure loss.

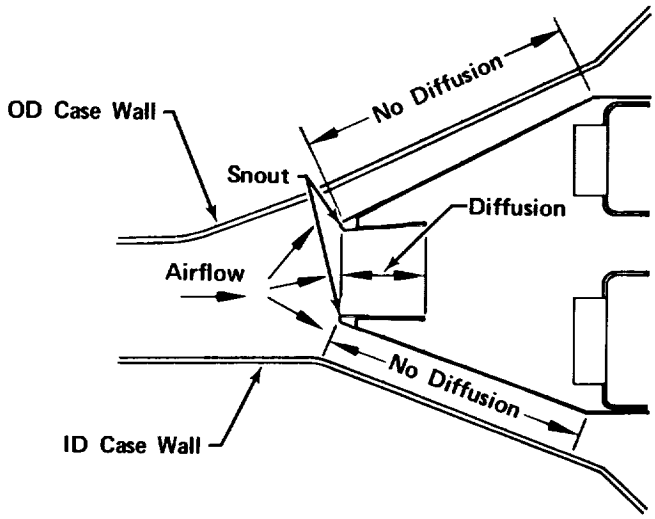

Figure 23a. 7-Degree ECA, Snout Type Diffuser

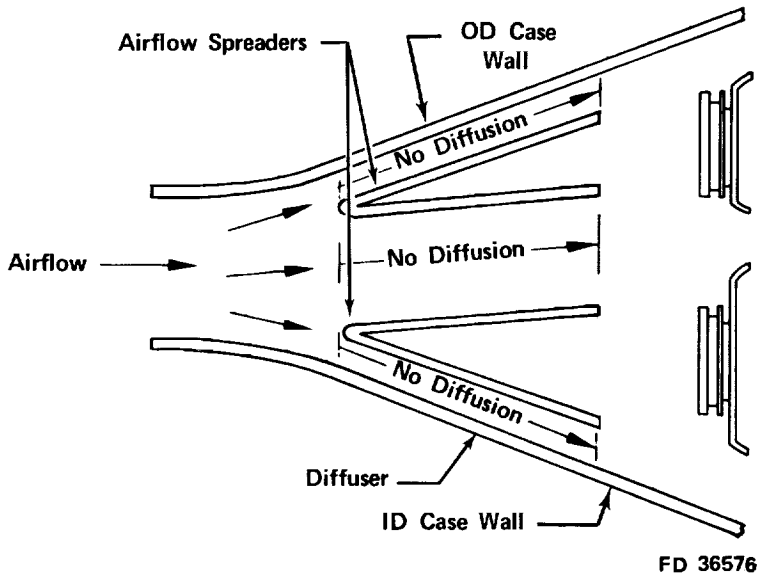

Figure 23b. 14-Degree ECA, Flow Spreader Diffuser

The circumferential temperature profiles, figures 24a and 24b, and temperature distributions, figures 25a and 25b, show that the temperature uniformity was better with the 7-degree (0.122-radian) ECA diffuser. Assuming a uniform fuel distribution for both configurations, one may infer that a more uniform airflow was obtained with the 7-degree (0.122-radian) ECA diffuser. This is demonstrated in the improvement of the temperature pattern factor from 0.21 for the 14-degree (0.244-radian) ECA diffuser to 0.18 for the 7-degree (0.122-radian) ECA diffuser.

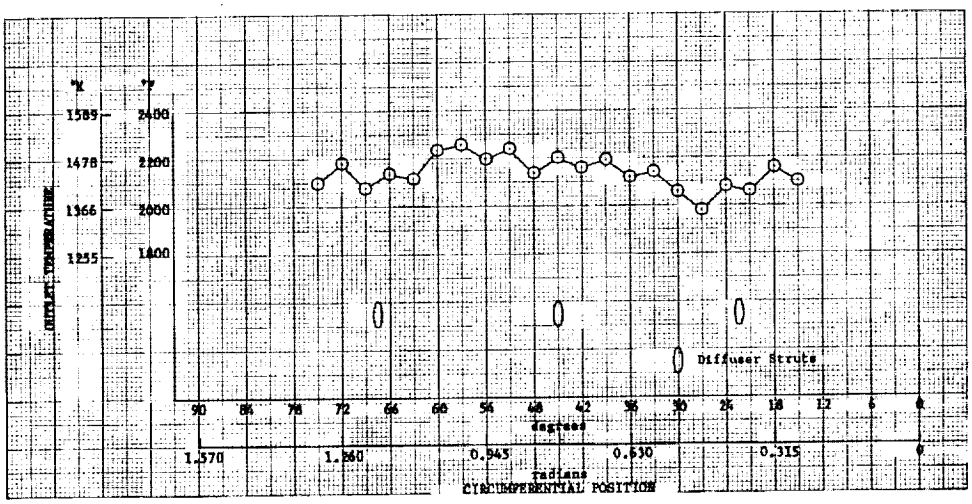

DF 79992

Figure 24a. Outlet Circumferential Temperature Profile, Model 1 Combustor Installed in 7-Degree ECA, Snout Type Diffuser

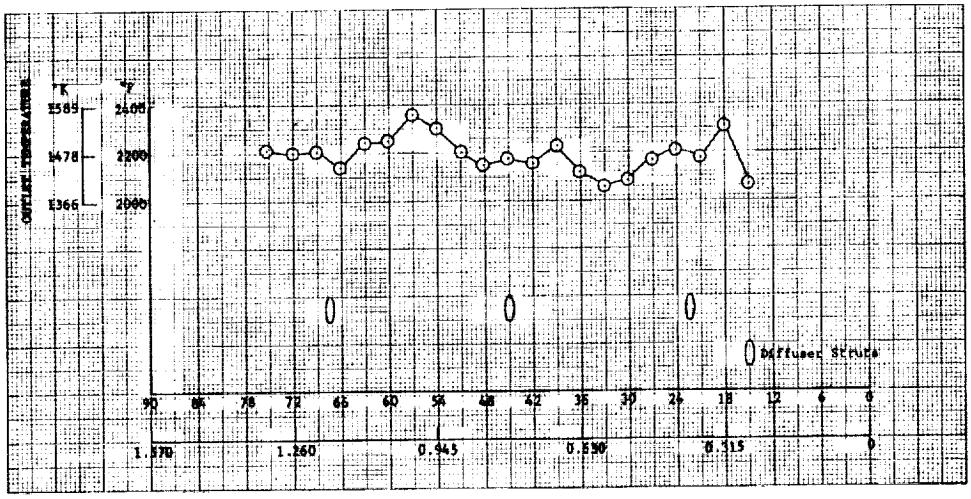

DF 79993

Figure 24b. Outlet Circumferential Temperature Profile, Model 1 Combustor Installed in 14-Degree ECA, Splitter Type Diffuser

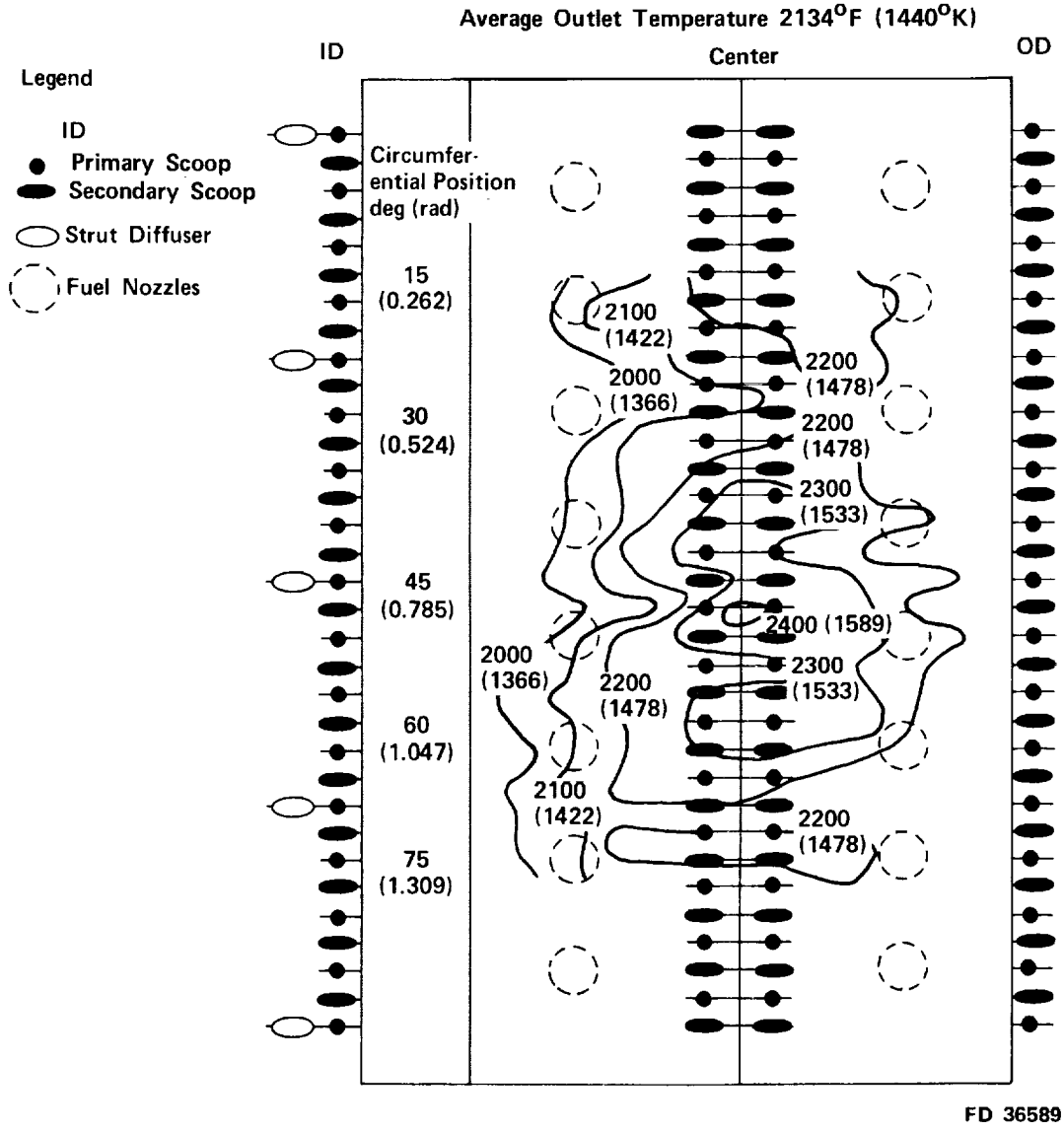

Figure 25a. Outlet Temperature Distribution, Model 1 Combustor Installed in 7-Degree ECA Diffuser

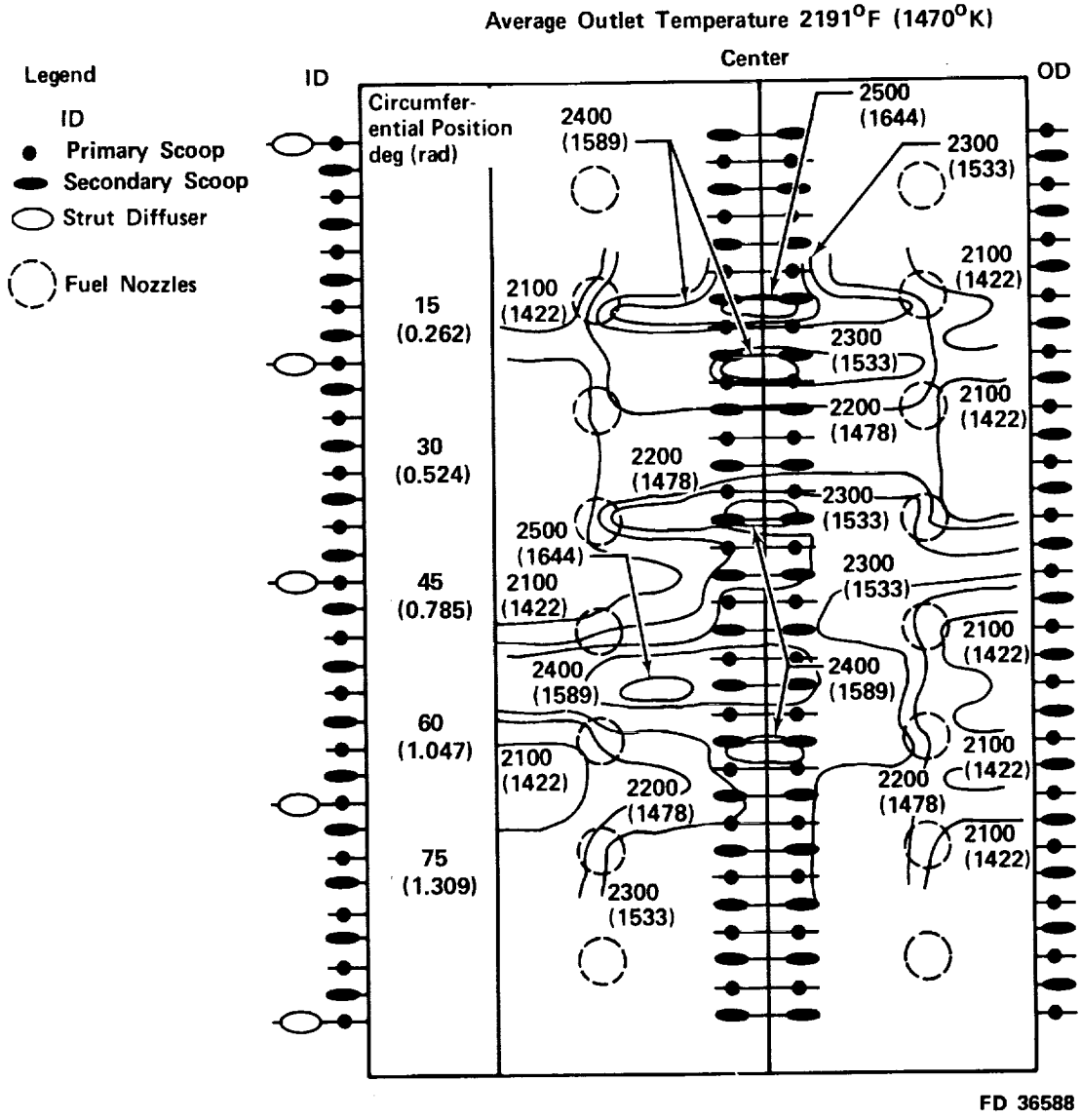

Figure 25b. Outlet Temperature Distribution, Model 1 Combustor Installed in 14-Degree ECA Diffuser

Performance Effects of Swirler Configurations. - Radial inflow and axial flow fuel nozzle air swirlers were investigated. Each configuration (figures 26a and 26b) was tested in the Model 1 combustor. Use of the axial flow swirler resulted in poorer outlet temperature uniformity. The temperature pattern factor increased to 0.29 from 0.21 with the axial flow swirlers installed. The combined diffuser-combustor total pressure loss increased slightly from 5.1% to 5.5% using the axial flow swirlers. Combustion efficiency was unaffected.

Ground Start Ignition. - Ignition studies were conducted with combustors using both the radial inflow and axial flow swirlers. A 20-Joule spark ignition system was used in all of the tests. The igniters were located

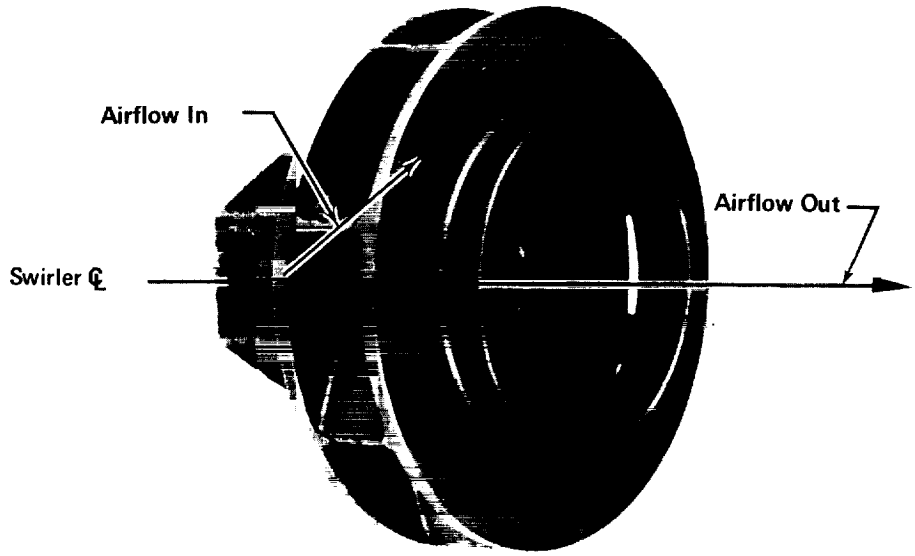

FE 92893
FD 36586

Figure 26a. Radial Inflow Fuel Nozzle Air Swirler

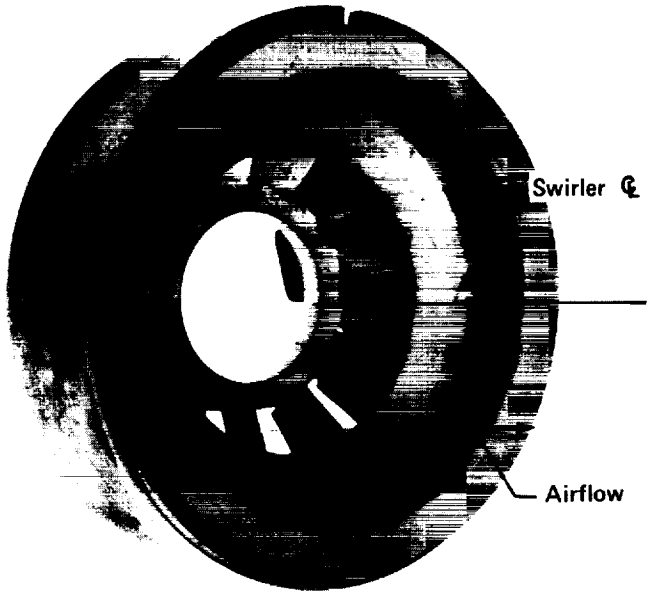

FE 97991
FD 36608

Figure 26b. Axial Flow Fuel Nozzle Air Swirler

in both the outer and inner annuli at various axial positions as shown in figure 27. The combustor inlet Mach number and temperature were set to simulate engine ground start conditions (inlet Mach number = 0.150; inlet-air temperature = 100°F (310.9°K)).

No difference in ignition capability was noted with either the radial or axial flow swirlers. Also, the axial position of the igniter had no effect on ignition capability. Ignition consistently occurred at a fuel-air ratio of 0.009. The outer annulus would light at a slightly lower f/a than the inner annulus. However, flame crossover from the outer to inner annulus was never observed. This failure to cross ignite was due to the inability of the flame to propagate past the center liner. The problem was corrected by installing a modified secondary scoop (figure 28) in the center liner. This scoop incorporates a crossover tube between the inner and outer annuli. Tests by the NASA have demonstrated cross-ignition and no adverse effects on performance with this scoop installed.

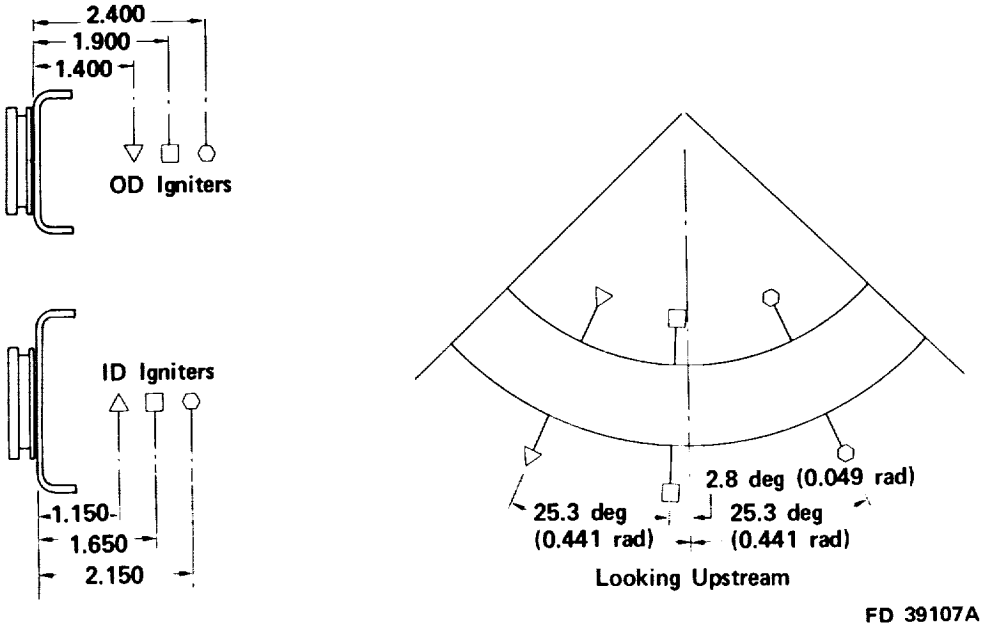

Figure 27. Igniter Positions

Test Effort in Support of NASA 360-Degree (6.282-Radian) Annular Combustor. - Concurrent with this 90-degree (1.57-radian) sector test program, the NASA is conducting tests on a 360-degree (6.282-radian) full annular combustor of similar design. The NASA program is being conducted at higher inlet air temperatures and pressures (1150°F (894.3°K) and 90 psia (62.05 N/cm^2)). Additional test effort to that described above was conducted on the 90-degree (1.57-radian) sector in support of the NASA 360-degree (6.282-radian) annular program. This effort was centered around diffuser airflow uniformity and firewall durability.

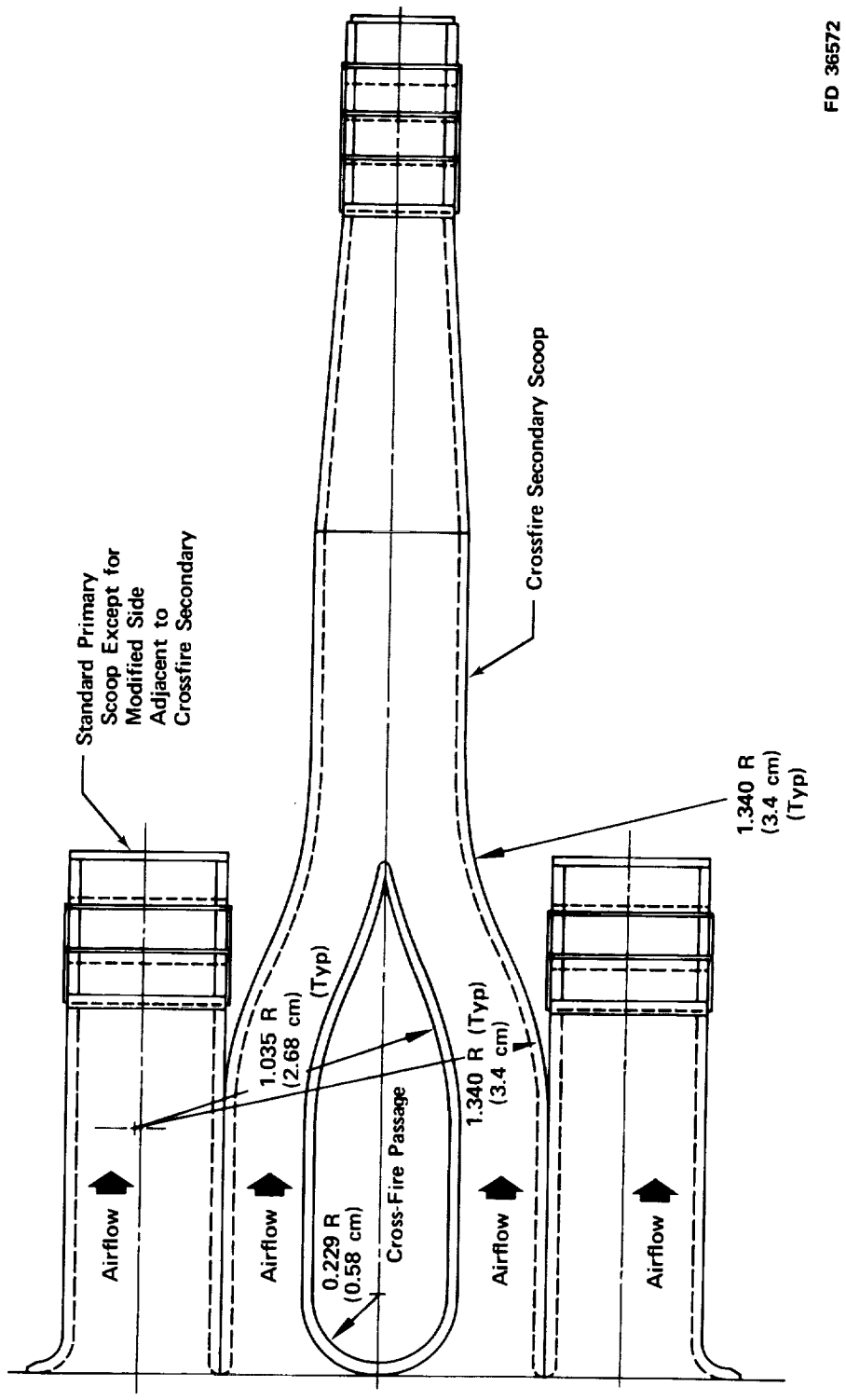

Figure 28. Crossfire Center Liner Secondary Scoop (Plan View)

Diffuser Airflow Uniformity. - The original diffuser furnished to P&WA at the start of the test program is shown in figure 29. This diffuser had two sheet metal splitter plates to assist in preventing diffuser stall. Initial hot tests by the NASA and P&WA with this diffuser produced a circumferential temperature profile which had large hot regions located behind each diffuser strut (figure 30). This was indicative of airflow separation from these struts, assuming that a uniform fuel distribution existed. This problem was eliminated by incorporating the flow spreader shown in figure 23b. The flow spreader was designed to give the diffuser a constant flow area from the spreader inlet to exit. The circumferential temperature profile, figure 24b, obtained with this spreader installed shows that this modification did correct the problem. This spreader design also corrected the problem on the NASA 360-degree (6.282-radian) combustor. The diffuser with this improved flow spreader is the 14-degree (0.244-radian) ECA diffuser used with the various combustor configurations described previously.

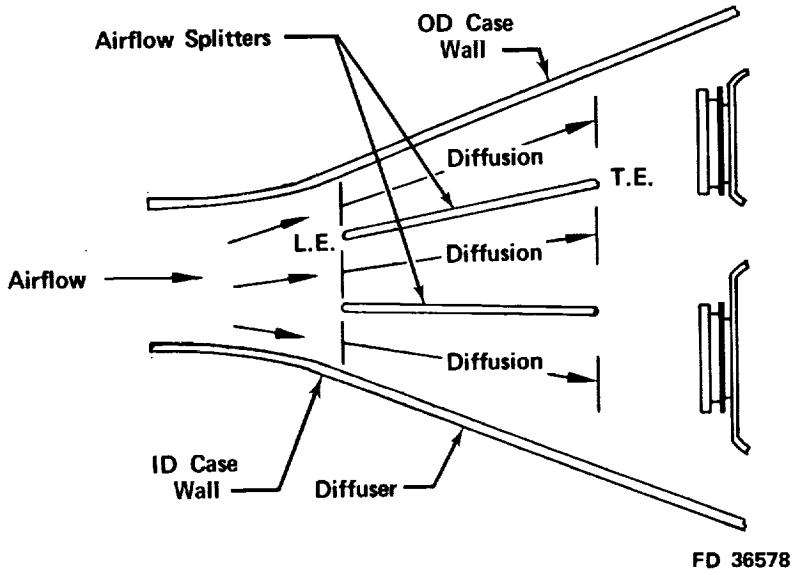

Figure 29. Initial Splitter Plate Diffuser

Firewall Durability. - The NASA test program showed that the combustor firewall was overheating at the 1150°F (894.3°K) inlet temperature condition. The affected areas were:

1. Both outer and inner firewall faces between fuel nozzles.
2. The center liner attachment lips immediately downstream of the rivet heads.

Figure 31 shows these locations.

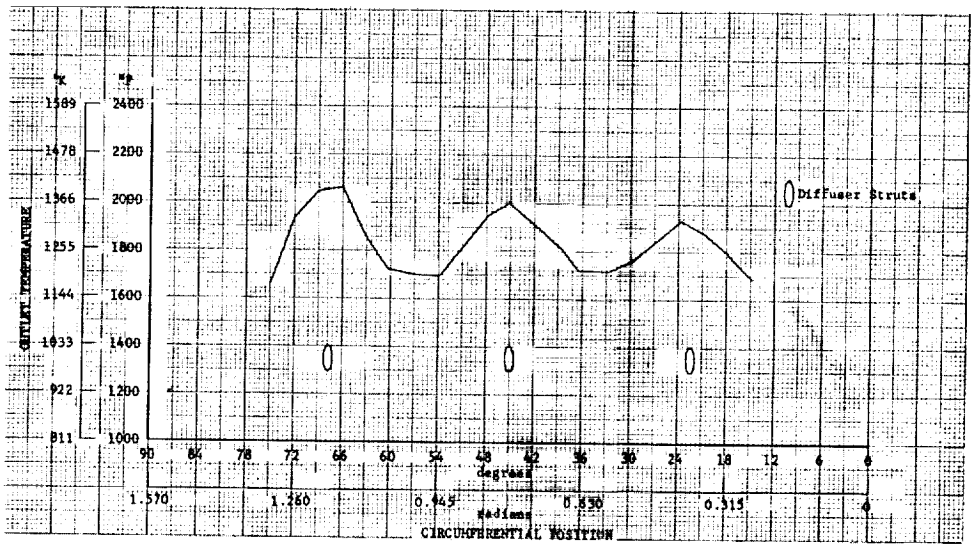

DF 79994

Figure 30. Outlet Circumferential Temperature Profile, Model 1 Combustor Installed in Initial Design Diffuser

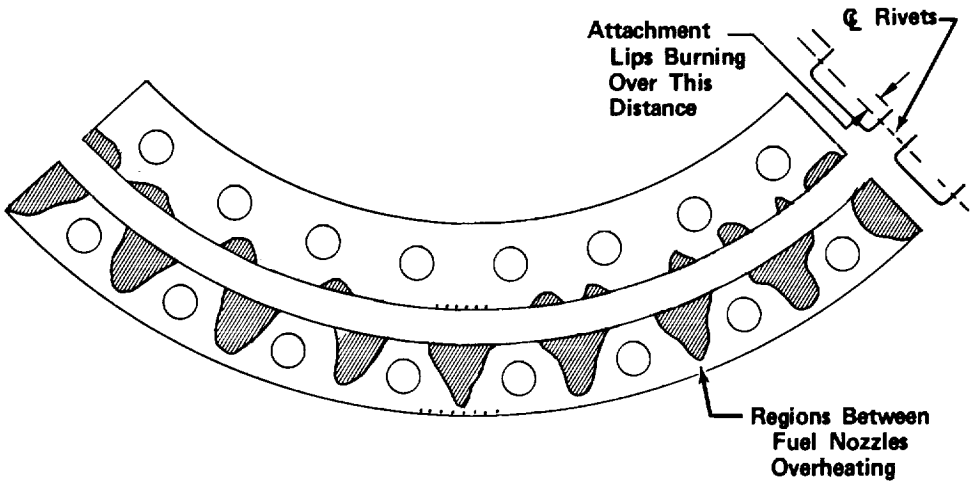

FD 29154A

Figure 31. Regions of Excessive Metal Temperatures, Initial Design Firewall

A partial solution was made by replacing the original deflector (figure 32) with the improved deflector shown in figure 33. The figures show that the improved deflector covered a larger area of the firewall face. To keep the new deflector from burning, the deflector flow area was increased by 230%. In addition, long slots in the firewall (figure 34) were incorporated to cool the center liner attachment lips. The increase in area at this location was 260%.

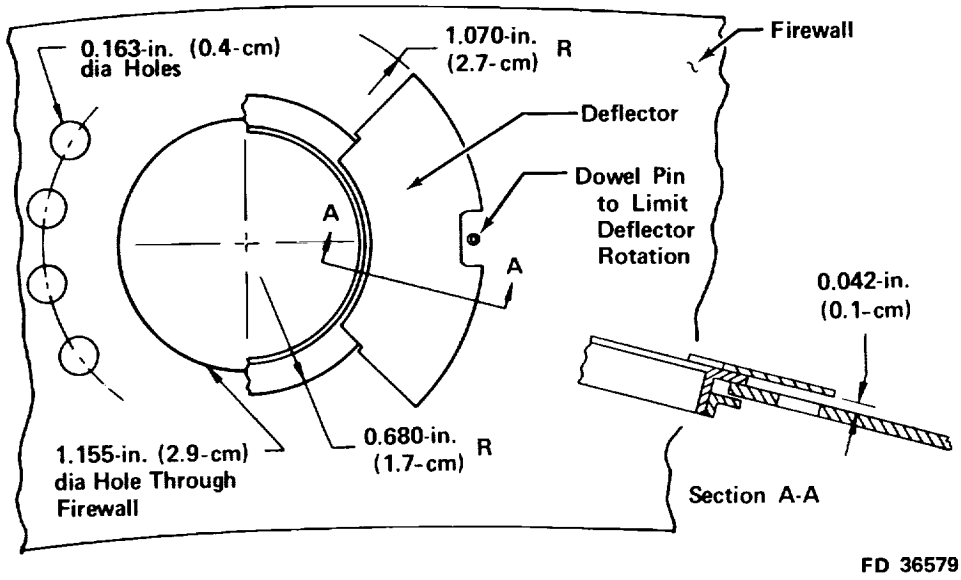

Figure 32. Initial Firewall Cooling Deflector Design

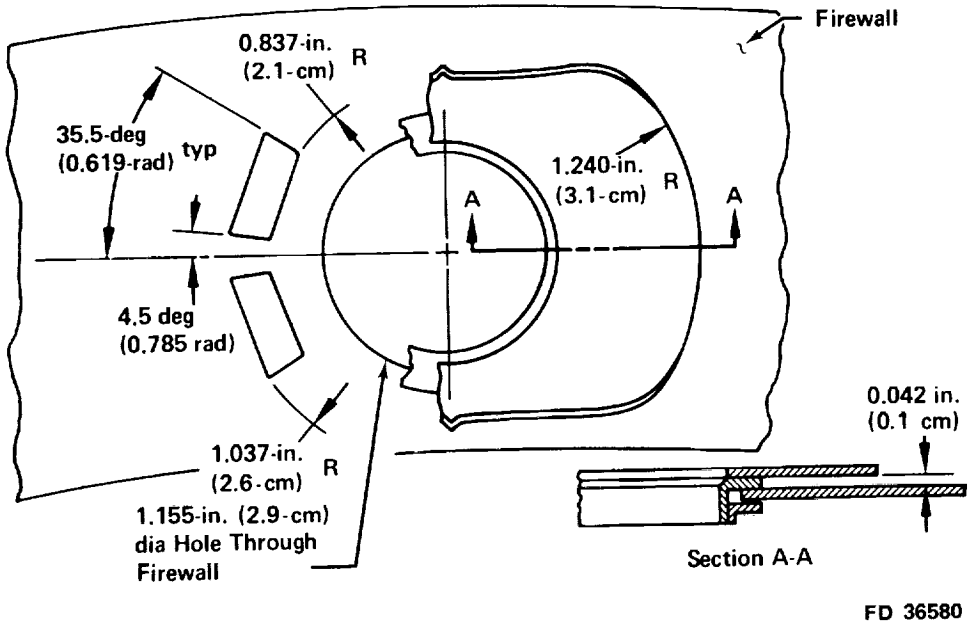

Figure 33. Final Firewall Cooling Deflector Design

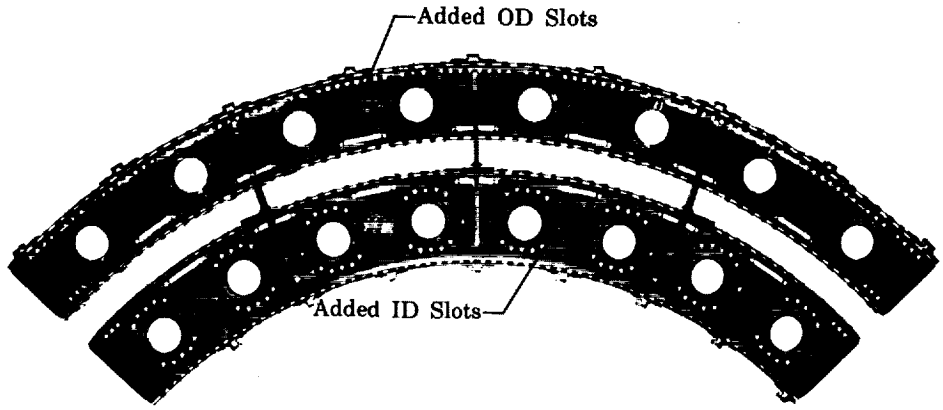

FE 87512
FD 33054

Figure 34. Improved Cooling Firewall

These modifications were only partially successful. The center liner attachment lips were still experiencing severe metal temperatures as of this writing (figure 35). Also, figure 35 shows that the corners of the deflectors burned; however, this may be corrected by trimming away that portion of the deflector. The improved deflector did reduce the metal temperatures of the firewall face to acceptable limits.

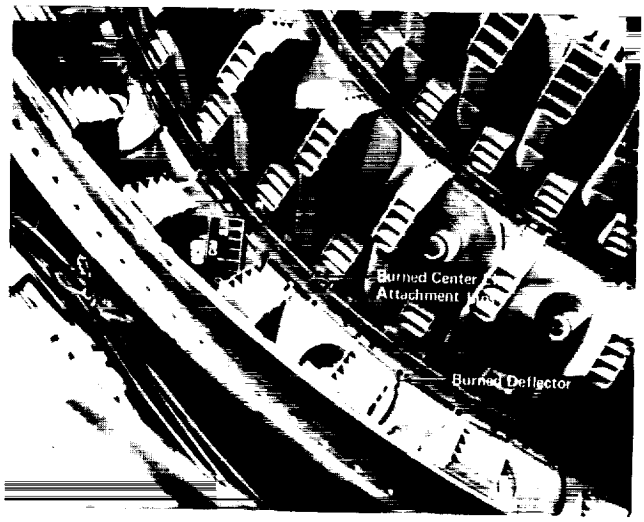

FD 36585

Figure 35. Firewall Damage Following Tests at 1150°F and 90 psia Inlet Temperature and Pressure

SUMMARY OF RESULTS

A performance test program was conducted on a double-annular, ram-inductor combustor, in a sector rig having 90 degrees (1.57 radians) of a full annulus. The test condition simulated the inlet air temperature 600°F (589°K), outlet temperature 2200°F (1478°K), and Mach number of a high flight speed, augmented turbofan engine during take-off operation. Testing was conducted at ambient pressure level, 16 psia (11.03 N/cm^2). The following results were obtained:

1. The double-annulus, ram-induction combustor concept demonstrated good performance. The best performance was obtained with a simplified design having one-half the number of air entry scoops as the initial design. Performance for this configuration is as follows:

   a. Temperature pattern factor (TPF) of 0.14.

   b. Outlet radial temperature profiles closely approximated a desired profile typical of advanced engines. In tailoring the profile to the desired shape, the dual annulus fuel system proved to be very effective.

   c. Combustion efficiency of nearly 100%.

   d. Total pressure loss of 5.6% at diffuser inlet Mach number of 0.244.

   e. Good ground start ignition capability. The combustors consistently ignited at a fuel-air ratio of 0.009 at inlet-air temperatures and Mach numbers simulating engine ground start conditions.

   f. Combustor performance unaffected by a moderate amount of diffuser inlet distortion.

2. The temperature uniformity and total pressure loss were adversely affected by changing the combustor primary to secondary area ratio from 0.75 to 1.00.

3. The temperature uniformity and total pressure loss were adversely affected by changing the ratio of the outer and inner liner to center liner scoop area from 1.50 to 2.50.

4. The circumferentially air-directed secondary scoops gave poor performance. This was primarily due to a severly center peaked radial profile.

5. The upstream air-directed secondary scoops gave a higher total pressure loss with no corresponding increase in outlet temperature uniformity

6. Cooling modifications made to the firewall were partially successful. The improved firewall deflectors eliminated the metal overheating on the firewall face. The temperature distress of the center liner attachment lips was not corrected.

7. Diffuser flow uniformity problems affecting circumferential temperature profiles were corrected by replacing the diffuser splitter plates with flow spreaders having no diffusion along their length. A further improvement was made by using a redesigned, snouted diffuser having a smaller diffusion angle.

8. Test results obtained with the sector rig compared well with the test results from a 360-degree (6.282-radians) annular combustor being tested by the NASA.

RECOMMENDATIONS

The following recommendations are made to point out areas needing additional effort:

1. Combined Diffuser-Combustor Total Pressure Loss - The total pressure loss of the double-annular, ram-induction combustor is high. In terms of the inlet dynamic pressure ($q = (1/2)\,\rho\,V^2$) the total pressure loss is 1.4q. State-of-the-art losses are in the range of 0.9 to 1.1q. The combustor open area should be increased to 263 in^2 (0.169 m^2) to bring the total pressure loss down to 1.0q.

2. Combustor Durability - Combustor durability is a major problem of this combustor at Mach 3 conditions. In addition to the firewall problems discussed above, the center liner has experienced severe overheating problems during high pressure testing by the NASA. More work needs to be done to alleviate these problems.

3. High Temperature Rise - The performance characteristics of the combustor operating at higher temperature rises should be investigated. Due to expected increases in turbine technology, temperature rises in the 2000°F (1111°K) to 2200°F (1222°K) range should be studied.

APPENDIX A

DESCRIPTION OF TEST HARDWARE

Combustor Configurations

The test liners were designed so that only modifications affecting the variable of interest were made. This minimized the performance side effects due to unrelated changes. In each configuration, other variables such as scoop discharge length to width ratios (L/W), total annulus air entry area, and liner cooling patterns were, where possible, identical to those of the Model 1 combustor design.

For those configurations where the scoop discharge areas or dimensions have been modified, a scoop size comparison is presented in table 2. All scoop discharge areas are taken as normal to the scoop discharge flow direction and are exclusive of scoop turning vane thickness.

Model 1. Initial Scoop Configuration. - These liners, figures 36, 37, and 38, have a total of 512 scoops in a 360-degree (6.282-radian) annular combustor. Each primary and secondary scoop row has 64 scoops in a full annulus. The outer and inner liner scoops are staggered in relation to the center liner scoops (figure 39). Since there are in each annulus 32 fuel nozzle positions in a full annulus, this scoop pattern repeats twice per nozzle spacing. All of the scoops turn the airflow into the combustor 90 degrees (1.57 radians) relative to the combustor axis.

Model 2. One-Half Number of Scoops. - This design, figures 40, 41, and 42, has half as many scoops of double the size of the Model 1 design. Like the Model 1, the scoop pattern is staggered in each row. However, because it contains half as many scoops, this pattern repeats only once per nozzle spacing.

Thumbnail scoops incorporated in the Model 1, outer and inner liners were made double size and positioned between scoops and in all secondary scoop ramps as in the Model 1 design.

Model 3. Increased Primary to Secondary Scoop Flow Area Ratio. - This design, similar to the Model 1 in appearance, had enlarged primary air entry scoops with correspondingly smaller secondary scoops. This configuration provided an increase of 32 and 37% in the respective inner and outer combustor annuli primary/secondary scoop area ratio over that of the Model 1. These particular values of area ratio increase were selected to allow use of the same primary scoop hardware in the Model 4 combustor.

Model 4. Increased Area Ratio of Outer and Inner Liner Scoops to Center Liner Scoops. - This design, similar in appearance to the Model 1, had enlarged primary and secondary scoops in the inner and outer liners with correspondingly smaller center liner scoops. The total scoop area was

Table 2. Scoop Sizes for Twin

Combustor Configuration	Standard Design	Increased Liner/ Shroud Flow De
Inner Annulus Entry Area Ratio		
Liner/Center Shroud	1.50	2.54
Primary/Secondary	0.74	0.74
Outer Annulus Entry Area Ratio		
Liner/Center Shroud	1.47	2.50
Primary/Secondary	0.75	0.75
Outer Liner Primary Scoop		
Discharge Area, in^2 (cm^2)	12.480 (80.496)	14.974 (96.58
Discharge Length/Width, in. (cm)	0.458/0.458 (1.163/1.163)	0.500/0.500 (1.270/1.270)
Outer Liner Secondary Scoop		
Discharge Area, in^2 (cm^2)	22.144 (142.829)	26.570 (171.3
Discharge Length/Width, in. (cm)	0.614/0.614 (1.560/1.560)	0.669/0.669 (1.699/1.699)
Outer Center Shroud Primary Scoop		
Discharge Area, in^2 (cm^2)	12.480 (80.496)	8.813 (56.84
Discharge Length/Width, in. (cm)	0.458/0.458 (1.163/1.163)	0.387/0.387 (0.983/0.983)
Outer Center Shroud Secondary Scoop		
Discharge Area, in^2 (cm^2)	11.072 (71.414)	7.810 (50.37
Discharge Length/Width, in. (cm)	0.614/0.306 (1.560/0.777)	0.520/0.259 (1.321/0.658)
Inner Center Shroud Primary Scoop		
Discharge Area, in^2 (cm^2)	12.480 (80.496)	8.794 (56.72
Discharge Length/Width, in. (cm)	0.458/0.458 (1.163/1.163)	0.387/0.387 (0.983/0.983)
Inner Center Shroud Secondary Scoop		
Discharge Area, in^2 (cm^2)	11.072 (71.414)	7.810 (50.37
Discharge Length/Width, in. (cm)	0.614/0.306 (1.560/0.777)	0.520/0.259 (1.321/0.658)
Inner Liner Primary Scoop		
Discharge Area, in^2 (cm^2)	12.544 (80.909)	14.560 (93.91
Discharge Length/Width, in. (cm)	0.481/0.438 (1.222/1.113)	0.517/0.469 (1.313/1.191)
Inner Liner Secondary Scoop		
Discharge Area, in^2 (cm^2)	22.720 (146.544)	27.660 (178.5
Discharge Length/Width, in. (cm)	0.773/0.490 (1.963/1.245)	0.850/0.539 (2.159/1.369)

Note: All areas are actual area for a full annulus.

Ram-Induction Combustor

Center sign	Increased Primary/Secondary Flow Design	Double-Size Design
	1.50 0.97	1.50 0.74
	1.47 1.03	1.47 0.75
2)	14.974 (96.582) 0.500/0.500 (1.270/1.270)	12.480 (80.496) 0.641/0.641 (1.628/1.628)
77)	19.650 (126.743) 0.579/0.579 (1.471/1.471)	22.144 (142.829) 0.856/0.856 (2.174/2.174)
4)	14.486 (93.435) 0.492/0.492 (1.250/1.250)	12.480 (80.496) 0.641/0.641 (1.628/1.628)
5)	9.066 (58.476) 0.558/0.278 (1.417/0.706)	11.072 (71.414) 0.856/0.427 (2.174/1.085)
1)	14.486 (93.435) 0.492/0.492 (1.250/1.250)	12.480 (80.496) 0.641/0.641 (1.628/1.628)
5)	9.066 (58.476) 0.558/0.278 (1.417/0.706)	11.072 (71.414) 0.856/0.427 (2.174/1.085)
2)	14.560 (93.912) 0.517/0.469 (1.313/1.191)	12.544 (80.909) 0.672/0.612 (1.707/1.554)
41)	20.704 (133.541) 0.739/0.468 (1.877/1.189)	22.720 (146.544) 1.083/0.686 (2.751/1.742)

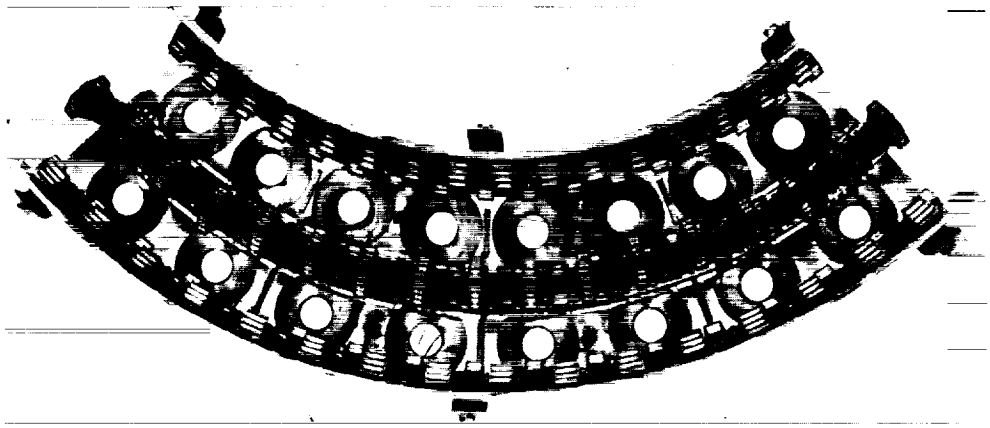

FE 91396
FD 36592

Figure 36. Assembled Model 1 Combustor

FE 98154
FD 36599

Figure 37. OD Liner, Model 1 Combustor

FE 98155
FD 36600

Figure 38. ID Liner, Model 1 Combustor

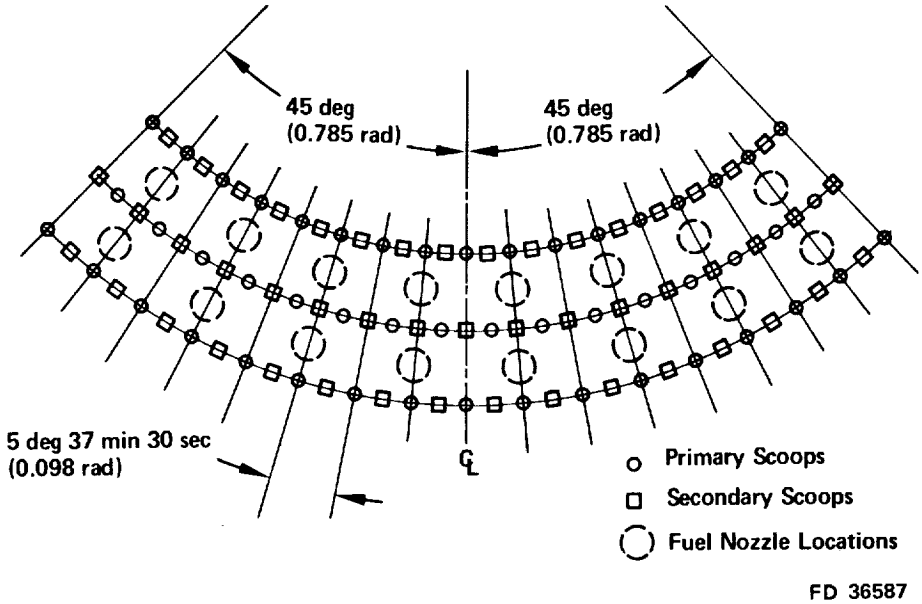

FD 36587

Figure 39. Scoop Pattern, Model 1 Combustor

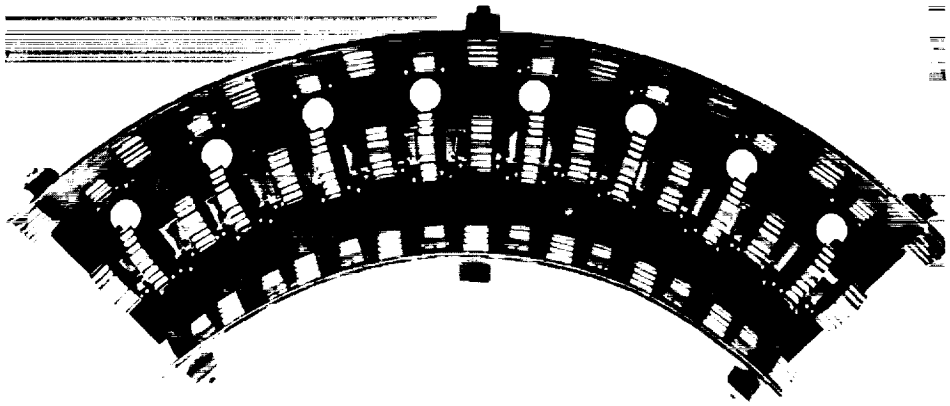

FE 89706
FD 36594

Figure 40. Model 2, 256-Scoop Combustor

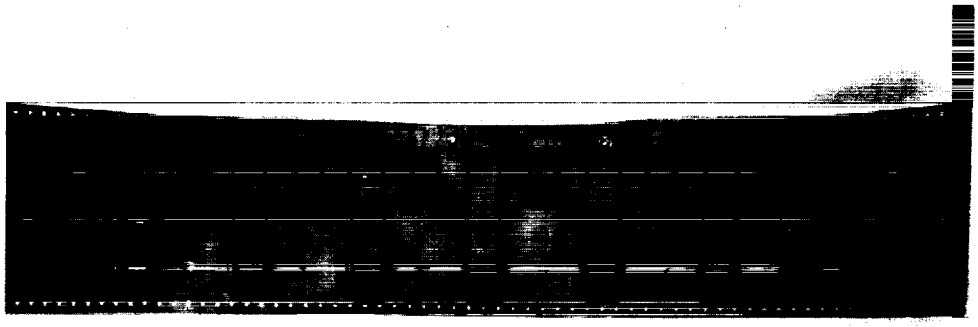

FE 89515
FD 36595

Figure 41. OD Liner, Model 2 Combustor

equal to the Model 1 design. This design provided an increase in area ratio of 67% over the Model 1. Using the Model 1 scoop discharge L/W, the ratio was limited to the 67% value by the circumferential clearance between the inner liner primary and secondary scoops.

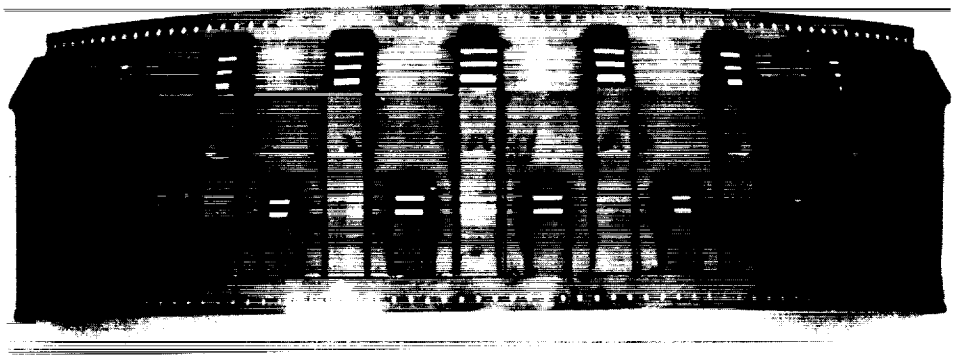

FE 89514
FD 36598

Figure 42. ID Liner, Model 2 Combustor

Model 5. Upstream Air Directed Secondary Scoop Design. - This design, figures 43 and 44, had revised secondary scoops which injected flow with a 45-degree (0.785-radian) upstream component rather than the full radial injection of the Model 1. The scoops had the same discharge area as those of the standard design. However, the scoops incorporated airfoil turning vanes to provide a constant area flow passage over the large 135-degree (2.356-radian) turning angle.

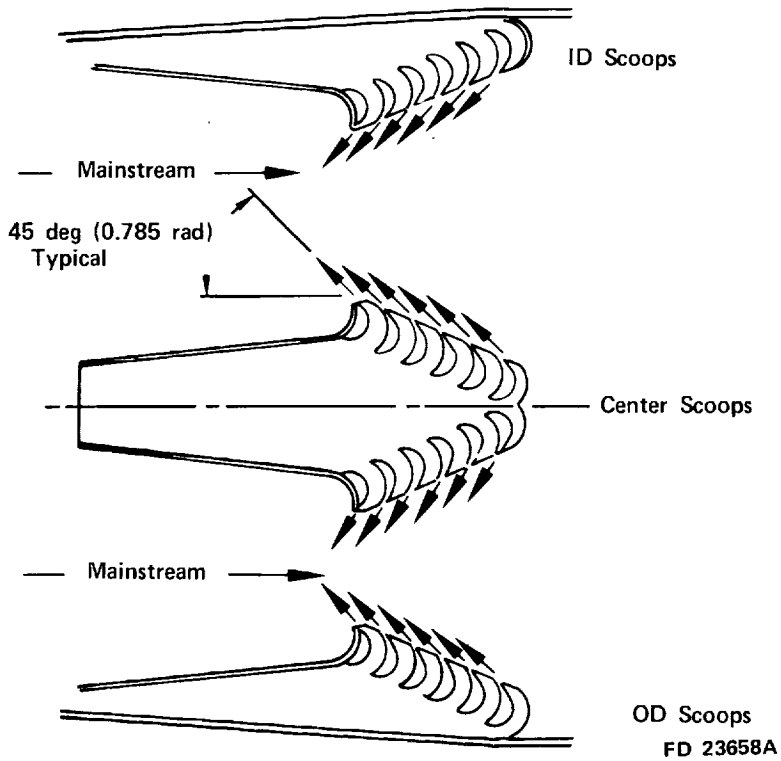

Figure 43. Upstream Air Directed Secondary Scoop Design, Model 5 Combustor

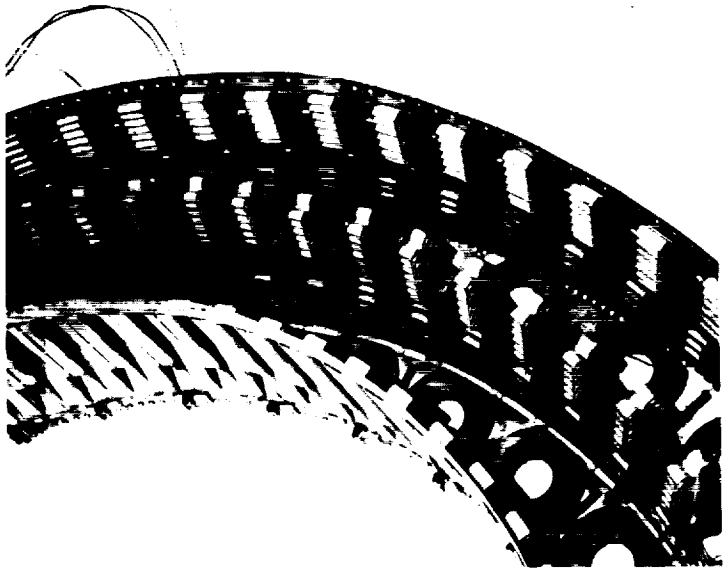

FE 96874
FD 36593

Figure 44. Model 5 Combustor

Model 6. Circumferential Air Directed Secondary Scoop Design. - This design, figures 45, 46, and 47, had revised secondary scoops which injected flow with a 45-degree (0.785-radian) circumferential component. All of the scoop discharge dimensions were the same as the Model 1. The thumbnail scoops in the secondary scoop ramps were positioned slightly farther upstream than those of the Model 1. In the assembled combustor, the secondary scoops were arranged so that the center liner circumferen-

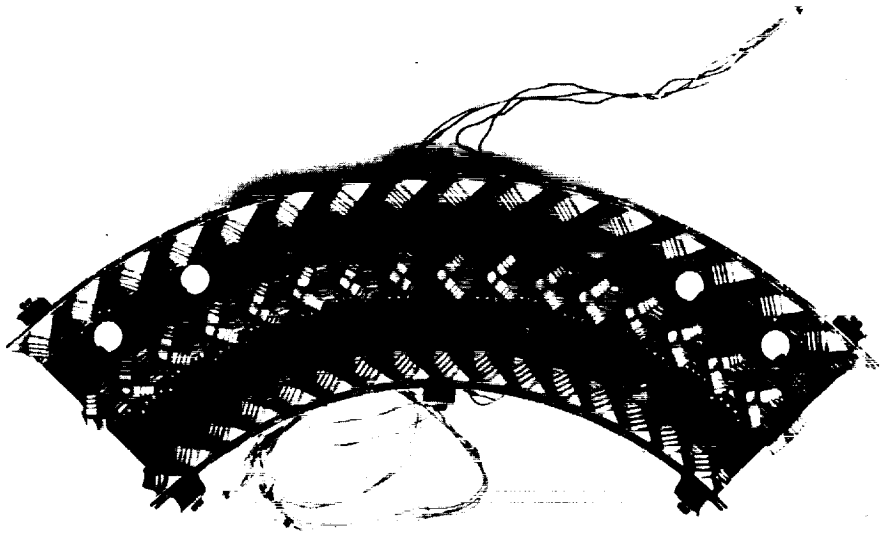

FE 89667
FD 36606

Figure 45. Model 6 Circumferential Air Directed Secondary Scoop Combustor

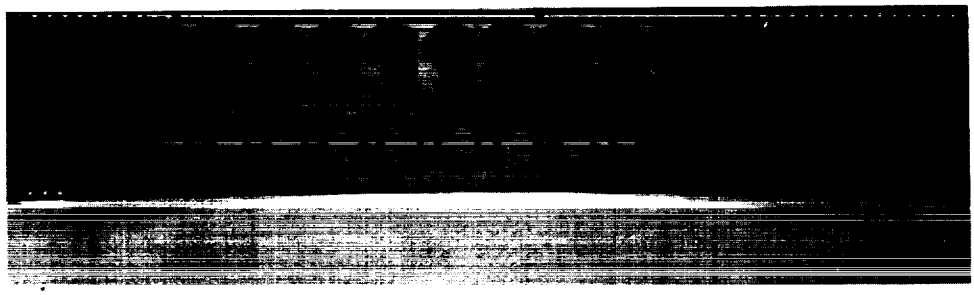

FE 89513
FD 36602

Figure 46 OD Liner, Model 6 Combustor

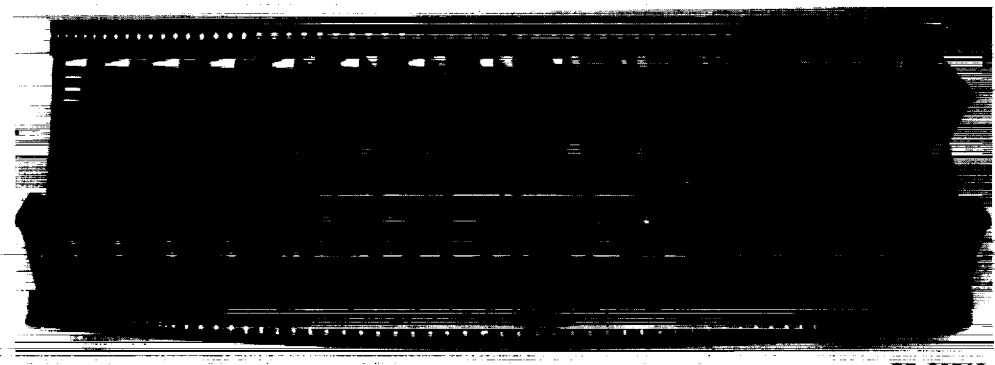

FE 89512
FD 36603

Figure 47. ID Liner, Model 6 Combustor

tial flow component opposed the outer and inner liner component (figure 48). This minimized the influence of the sector end walls. If the flow components were not opposed but in the same direction, a circumferential swirl would result. That arrangement can be evaluated in the 360-degree (6.282-radian) combustor but not in the sector.

Model 7. Opposed Scoop Design. - This design used the Model 1 liners except the center liner was rotated so that all of the corresponding primary and secondary scoops were opposed (figure 49).

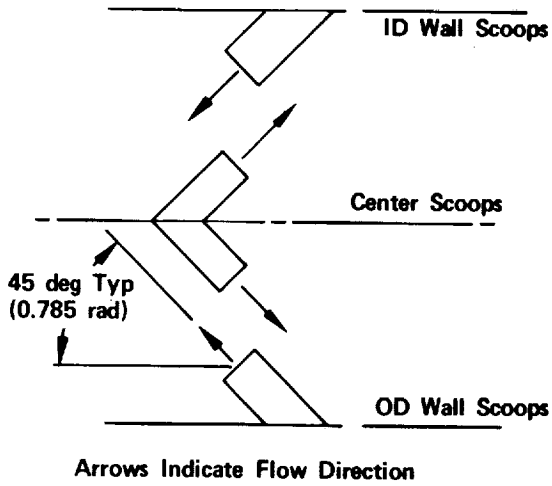

Figure 48. Secondary Scoop Arrangement, Model 6 Combustor

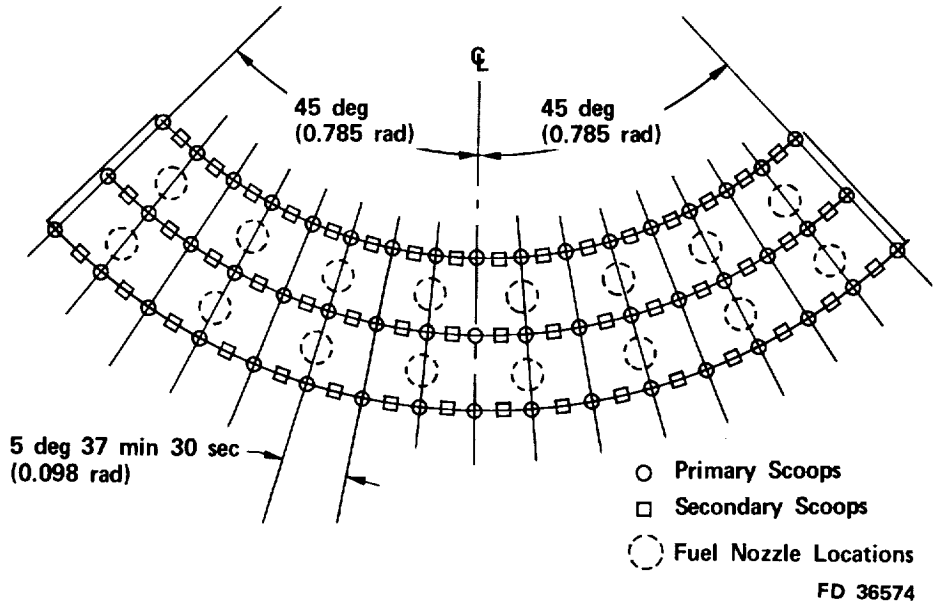

Figure 49. Opposed Scoop Pattern, Model 7 Combustor

Diffuser Configurations

7-Degree (0.122-Radian) ECA Snouted Diffuser Design. - This diffuser design incorporated, where possible, several general features shown to be desirable from performance investigations conducted at Pratt & Whitney Aircraft's Florida Research and Development Center. These features are as follows:

1. The diffusion rate should be conservative, with an equivalent conical angle (ECA) of 7 degrees (0.122 radian) or less in the diffusion passages to provide non-separated, uniform flow to the combustor.

2. The leading edges of flow spreaders or combustor snouts should be located downstream of the diffusion process, if possible, to minimize sensitivity to variations in inlet velocity profile.

3. The snout center flow passage opening should be sized to accept flow at a velocity that is nearly equal to the approach velocity to improve overall pressure recovery of the diffuser.

4. Any turns in the flowpaths, from the leading edge of the spreader or snout to the combustor shroud entrances, should be made so that no diffusion occurs in these passages.

5. The flow should be accelerated slightly at the combustor shroud entrance to reduce variations in the flow distribution at these points.

Following these criteria, diffusion in this design occurred only between the diffuser inlet and the snout leading edge, which is a distance of 3.605 inches (0.092 m). The diffusion passage was designed so that diffusion occurred at an equivalent conical angle of 7 degrees (0.122 radian).

This rate of diffusion resulted in an area ratio of 1.235 based on an inlet area of 184.32 in^2 (0.119 m^2). The snout inlet wall radii were positioned so that the total exit flow area was apportioned according to the combustor area splits, which were:

Outside diameter passage = 23.7% (total area)

Center passage = 53.3% (total area)

Inside diameter passage = 23.0% (total area)

The snout outside and inside diameter walls were then contoured to provide a smooth transition to the outer and inner combustor liners. A prime consideration in arriving at an outer wall contour was the sealing requirements between the fuel nozzle support struts and the snout walls. These requirements coupled with manufacturing simplicity dictated the use of conical wall sections. A very large opening in the snout outer wall was required to clear both the radial and axial flow swirlers when installing the fuel struts. The large sheet metal plate on the fuel nozzle support strut (figure 50) was designed to seal the opening in the snout wall, and to present a smooth surface to the airflow in that passage.

The center passage in the flow spreader was extended 1.6 inches (0.041 m) downstream from the inlet. Some additional diffusion was incorporated to reduce the dump losses associated with this passage.

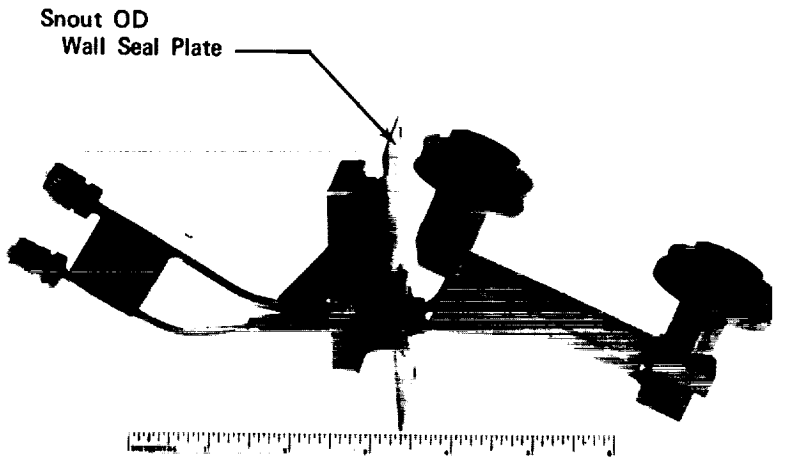

Figure 50. 7-Degree ECA Diffuser Fuel Strut Assembly

Downstream of the spreader inlet the case walls were contoured to provide no net area change. Some local diffusion and acceleration does occur in these passages due to the decreasing thickness of the diffuser struts. Figure 51, which is a plot of the flow area/pound airflow/second against diffuser length, shows the extent of local diffusion and acceleration in the outer and inner passages. The dip in the outer passage curve is due to the airfoil shaped fuel nozzle strut. A NACA 0012 airfoil section was selected for the fuel strut since it gave the minimum thickness needed to install the fuel tubes while maintaining a reasonable strut length. Figure 52 shows the exterior of the case outer wall. The fuel nozzle holes are elongated so that the fuel strut assembly can be moved upstream. This is necessary to disengage the swirler from the combustor firewall during disassembly. A spacer plate seals the opening after the fuel strut is installed. Figure 53 shows the final contour and gives all of the pertinent dimensions.

Swirlers

Radial Inflow Swirler. - The radial inflow swirler (figure 26a) was included in the initial design combustor system. It was designed to direct swirler air radially in toward the fuel nozzle center line. After mixing with the fuel the mixture was injected axially into the combustor through a 0.840-in. (0.021-m) diameter hole in the downstream face of the swirler.

The minimum effective flow area of this design was 0.395 $in.^2$ (2.55 cm^2) based on flow data supplied by the NASA. The C_d was determined to be 0.50.

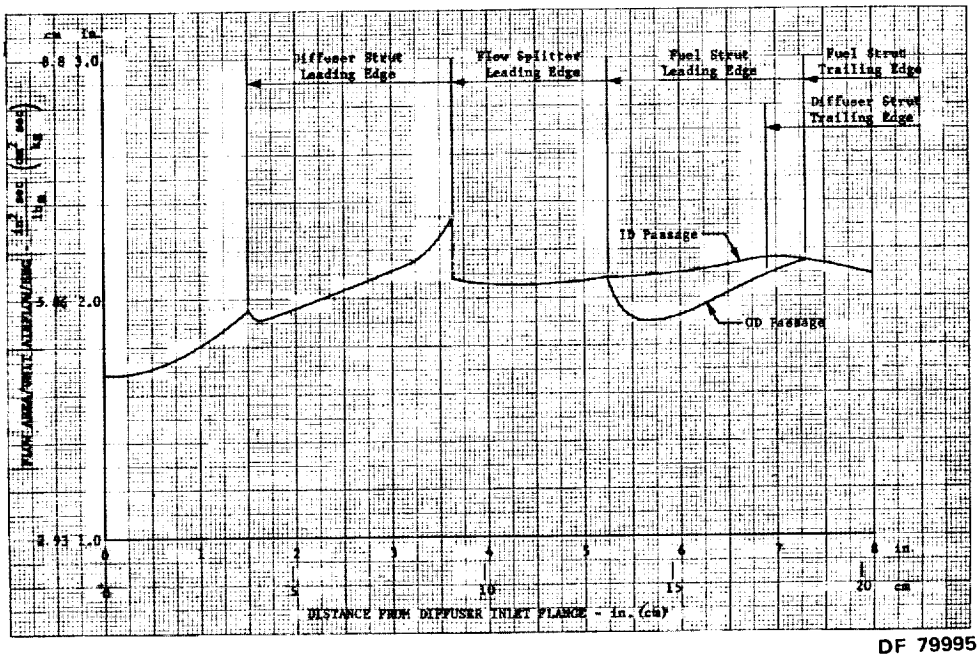

Figure 51. Variation of Diffuser Flow Area With Length

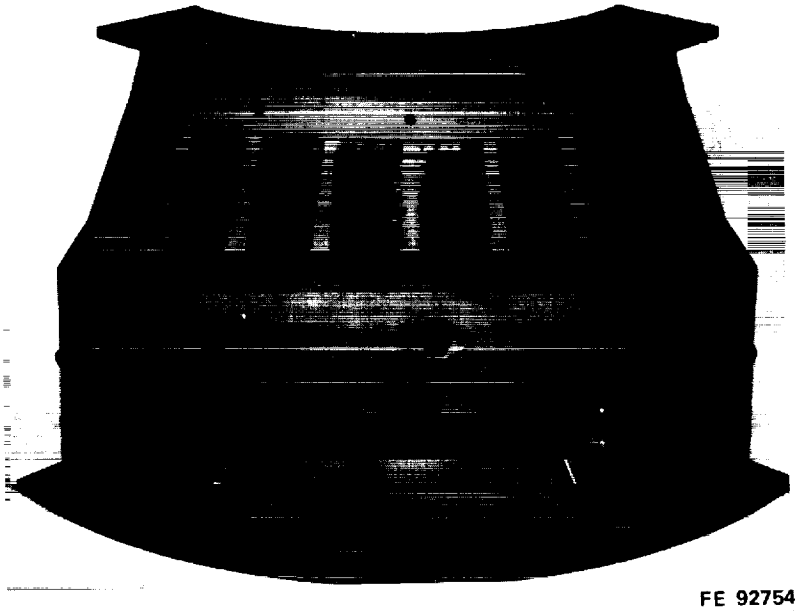

Figure 52. 7-Degree ECA Diffuser Case

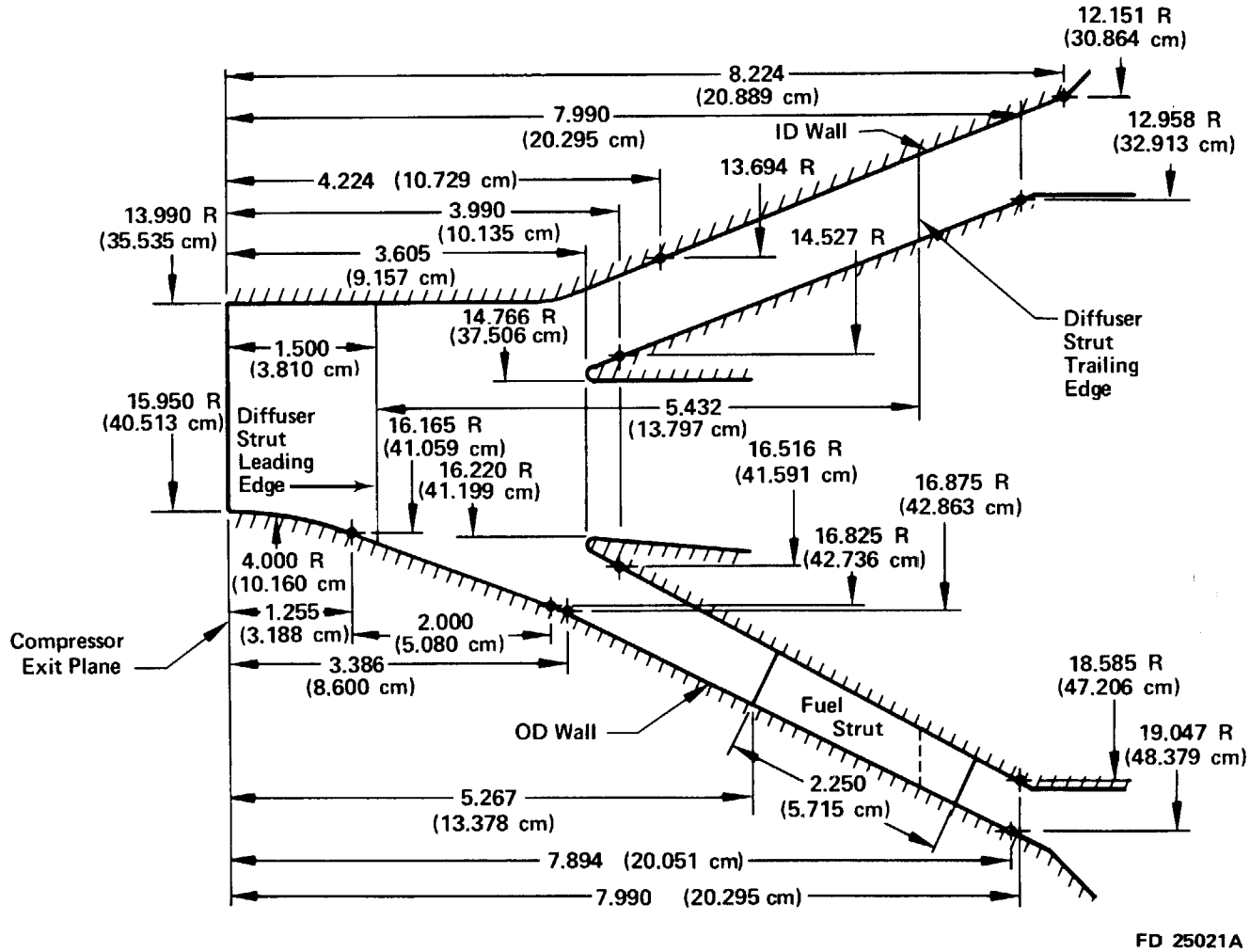

Figure 53. 7-Degree Diffuser Flow Passage Contour

The swirler is a one-piece assembly incorporating both the swirl housing and the fuel nozzle retaining nut. A flange on the downstream face of the swirler was designed to engage in a slipring device attached to the combustor firewall. This slipring functioned to seal the swirler to the firewall, while allowing for component tolerances and thermal growth during operation.

Axial Flow Swirler. - The axial flow swirler (figure 26b) was sized to have the same minimum effective airflow entry area as the radial inflow swirler design. The initial design C_d (0.5) was found to be too small (the measured C_d was 0.6) resulting in an effective flow area greater then the radial inflow swirler. The blockage plate shown in the figure was installed to equalize the flow areas of the two designs.

The axial swirler design featured twelve turning vanes so that there was a slight overlap of the leading edge of one vane and the trailing edge of the succeeding vane. A seal ring arrangement was used between the swirler and the firewall to allow for component tolerances and thermal growth during operation.

The axial swirler assembly was comprised of two units as compared to the single-piece radial inflow swirler. One unit was the fuel nozzle retaining nut and the other the air swirler itself. The two-piece design permitted removal of the large diameter swirl housing from the fuel nozzle strut without disturbing the fuel nozzle seal. This allowed installation of the nozzle holder through the openings in the 14-degree (0.244-radian) ECA diffuser case; the swirl housing was too big to pass through the opening. On assembly, the two swirler pieces were secured with a simple snapring. An integral tab on the swirler unit provided an anti-rotation lock.

Fuel Nozzle Flow Specifications

The nozzle flow specification was based on testing at simulated cruise conditions [T_{t3} = 1150°F (894°K); T_{t4} = 2200°F (1478°K)] ; a diffuser inlet pressure of 16.2 psia (11.17 N/cm^2) was assumed. The nozzles, figure 54, were simplex nozzles sized to allow a variable flowrate in the outer and inner annuli to control the exit temperature profile. An outer/inner annulus fuel flow ratio of 1.15 was assumed as the limit of unbalance based on double-annular, ram-induction combustor experience (reference 1). A fuel nozzle ΔP of 150 psi (103 N/cm^2) was specified to provide adequate atomization at the minimum cruise flowrate of 17 pph (7.71 kg/hr) per nozzle, which would occur in the inner annulus when running the 1.15:1 flow split. The maximum flowrate was 32 pph (14.51 kg/hr) per nozzle which occurred in the outer annulus when running the 1.15:1 flow split at sea level conditions. The nozzle ΔP at this condition was approximately 530 psi (365 N/cm^2).

External dimensions of the fuel nozzles were identical to those used in the NASA 360-degree (6.282-radian) annulus combustor program.

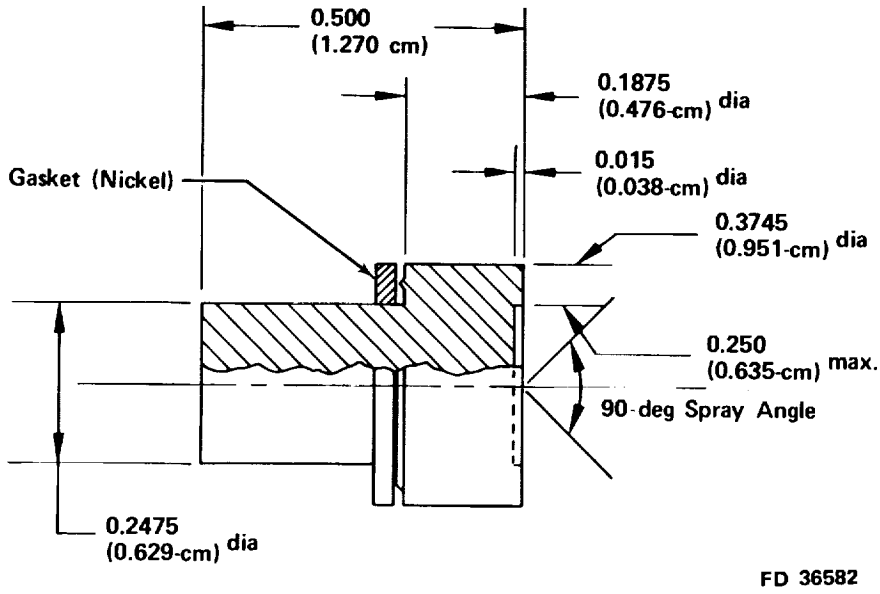

Figure 54. Fuel Nozzle (Dimensions in Inches)

APPENDIX B

TEST FACILITY AND TEST RIG DESCRIPTION

Test Facility. - All combustion tests were conducted on test stand D-33B at the P&WA Florida Research and Development Center. Combustion air was supplied by bleeding the compressor discharge of a JT4 turbojet engine. Airflow rate was controlled by a pneumatically operated 10-inch (25.4-cm) inlet butterfly valve with vernier control by a 4-inch (10.16-cm) pneumatically operated supply line bleed valve.

The test stand fuel system was capable of supplying each of three combustion zones with 300 pph (136.08 kg/hr) of ASTM-A1 type fuel at 750-psig (517-N/cm^2) fuel pressure. Control room monitoring of fuel pressure and temperature was provided for each zone.

The test facility had high pressure steam service available to operate steam ejectors. The ejectors were needed to aspirate the outlet temperature traverse probe.

Test Rig Description. - A brief description of the major components of the combustor test rig is presented below. For reference, a cross section of the rig is presented in figure 55 and the rig installation in the D-33B test facility in figure 56. The rig was constructed entirely of AISI type 347 stainless steel.

Flow Straightener. - This section was designed to smooth out any irregularities in rig inlet airflow and to provide a near stagnation region for accurate measurement of inlet total pressure and temperature. The flow straightener was fabricated from a 12-inch (30.480-cm) diameter cylinder 24 inches (60.960 cm) long. A bank of 1.5-inch (3.81-cm) diameter tubes 12 inches (30.480 cm) long was used to straighten the inlet airflow.

Venturi. - This section provided accurate airflow measurement with minimum pressure loss. The rig airflow entered through a constant radius inlet to a 4.7483-inch (12.0607-cm) diameter throat. Since the throat measurement was made at 71°F (294.8°K) a coefficient of linear expansion of 12 x 10^{-6} in./in.-°F (21.6 x 10^{-6} cm/cm-°K) was applied to correct the throat diameter at higher temperatures. Transition from the venturi throat to the preheater inlet was provided by a conical diffusing section 40.840 inches (103.7 cm) long with a 12-degree, 31-minute (0.218-radian) included angle.

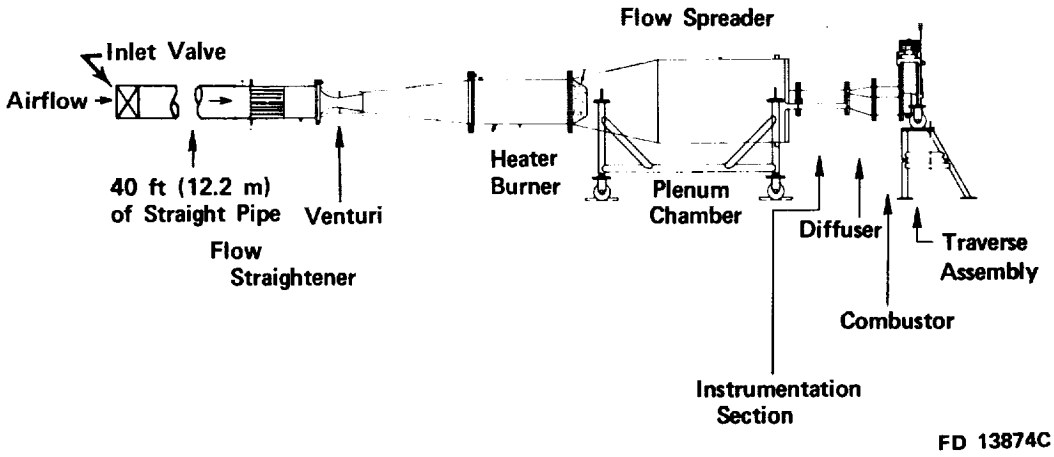

Figure 55. Double-Annular Combustor Test Rig

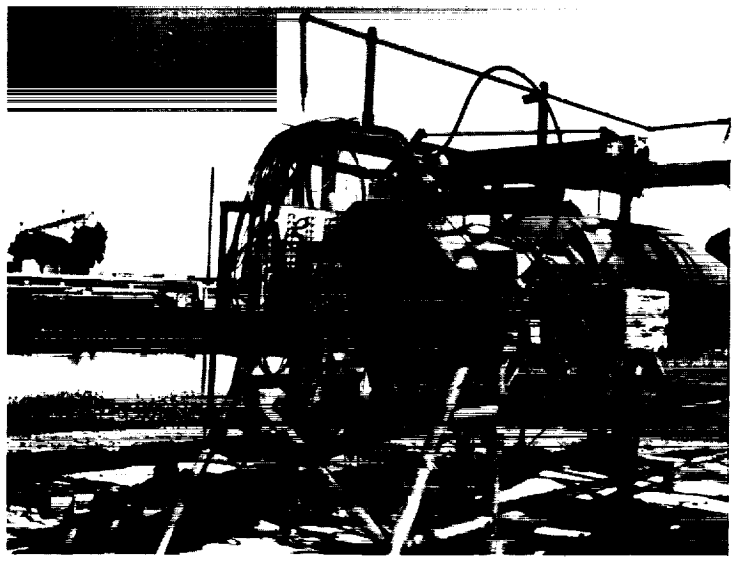

Figure 56. Test Rig Installation, D-33B Test Stand

Preheater. - The preheater assembly provided the capability of supplying vitiated combustion air to the combustor at temperatures from ambient to 1150°F (894°K). It was fabricated from a cylindrical housing 12 inches (30.480 cm) in diameter and contained a modified combustor from a turbojet engine. The preheater fuel nozzles were sized to give good atomization for use in an ambient pressure level rig.

Plenum Chamber. - The plenum chamber functioned to provide airflow to the rig test section at uniform temperature and pressure. This was accomplished by discharging the airflow from the preheater through a multihole flow spreader into a large volume container. The plenum was fabricated from a cylinder 29.250 inches (74.295 cm) in diameter and 48 inches (121.920 cm) long. To ensure a uniform profile into the rig test section, a bellmouth flange was incorporated to transition from the plenum exit area to the test section inlet area. Bosses were installed near the exit of the plenum for the installation of temperature sensors to measure the combustor inlet temperature.

Instrumentation Section. - This section housed the instrumentation used to determine the diffuser inlet total pressure, static pressure, and pressure profiles. It was designed to simulate a quarter section of the compressor discharge of a full-scale engine.

Diffuser-Combustor Case. - This section housed the combustor hardware and functioned to direct the inlet airflow into the combustor liners.

Traverse Case. - This section provided a platform for the combustor outlet traverse probe and actuating mechanism. The case also functioned as a rear support for the test rig.

Cold Flow Survey, Test Section Inlet. - A total and static pressure survey of the test section inlet was made to determine if any rig-induced flow irregularities existed at the diffuser inlet.

The pressure survey was obtained with the 5-point pressure survey rake shown in figure 57. The rake sensors were radially spaced to provide equal area sampling. The center probe was a pitot-static tube so that the static pressure at each circumferential position could be determined. The rake was positioned so that the sensor tips were approximately 1.0 inch (2.54 cm) downstream of the trailing edge of the regular instrumentation section rakes.

The test was conducted without the inlet airflow distortion screens so that rig-induced distrubances could be isolated.

The data from this inlet survey (figures 58 through 60) showed very little rig-induced flow irregularities at the diffuser inlet. The velocity head contour map (figure 58) showed the airflow to be quite uniform over most of the cross section. Only slight wakes were observed downstream of the permanent instrumentation section rakes (see figure 59). The radial profile from the survey rake (figure 60) was flat and almost symmetrical about the profile midpoint.

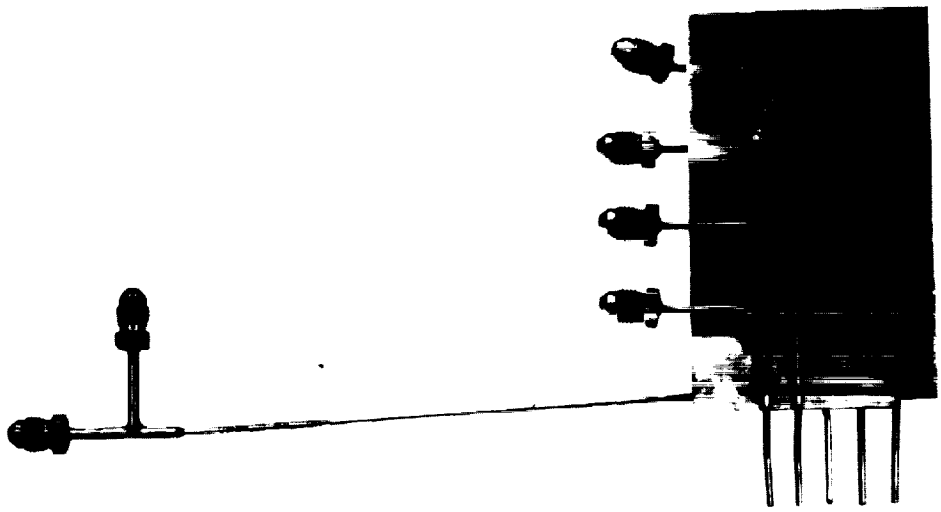

FE 92897
FD 36596

Figure 57. 5-Point Total Pressure Survey Rake

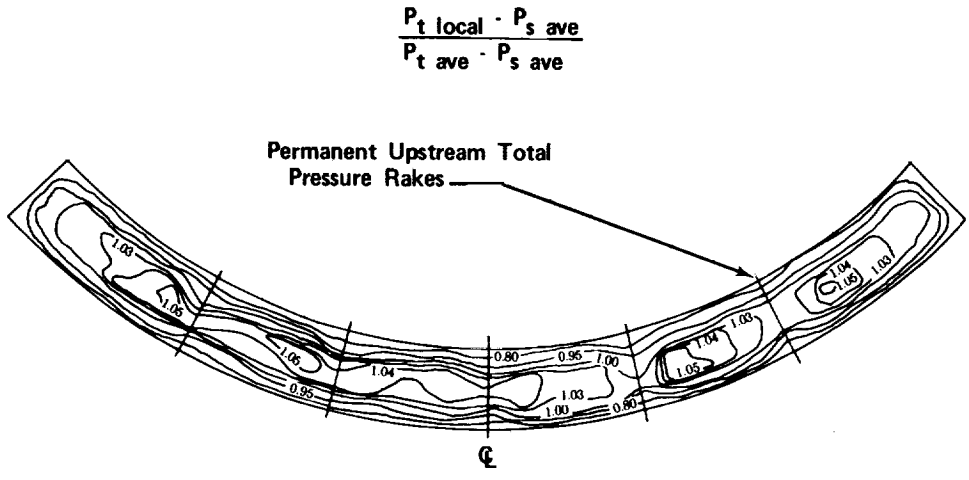

FD 27879A

Figure 58. Velocity Head Contour Map, Instrumentation Section Exit

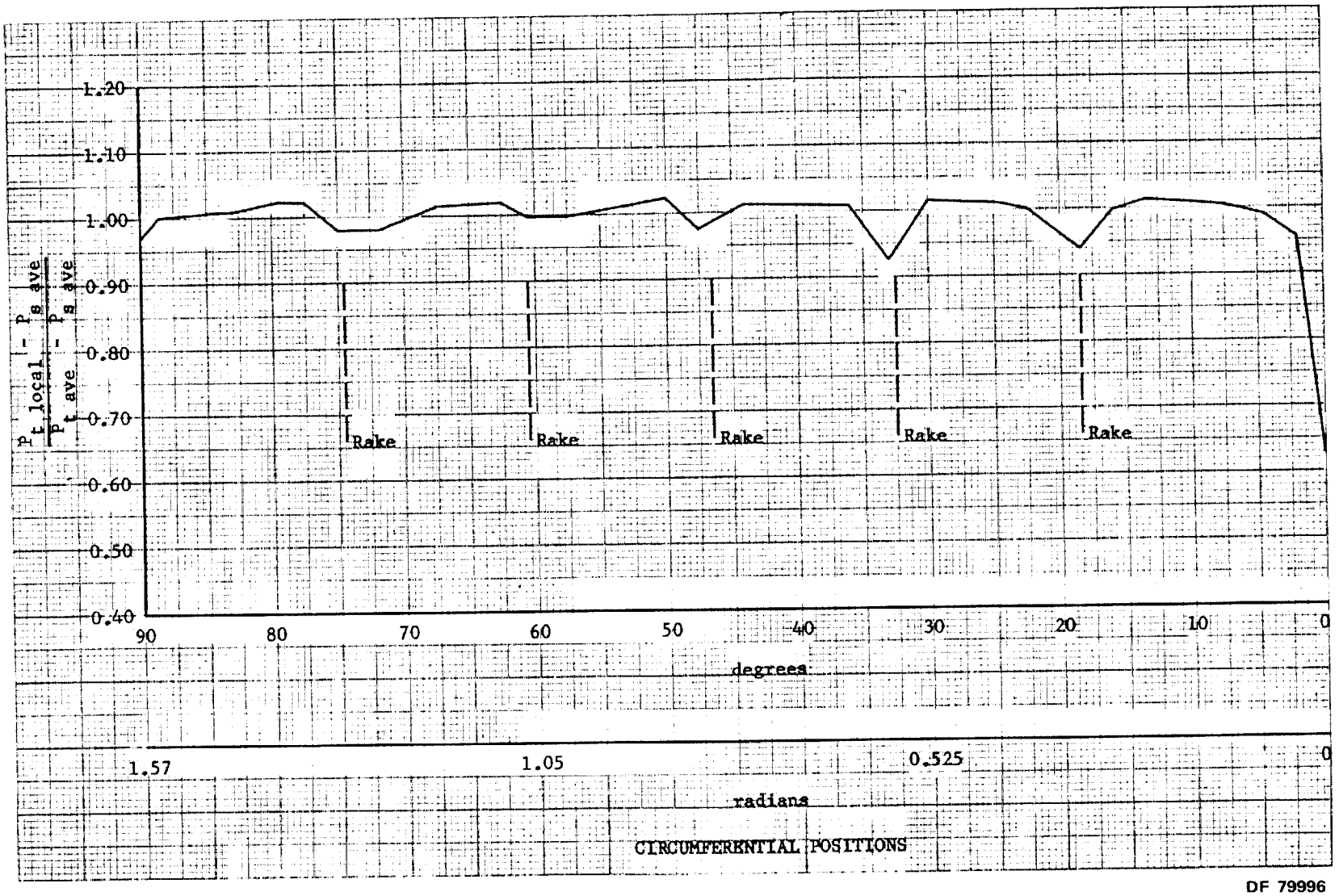

Figure 59. Circumferential Velocity Head Profile, Survey Rake

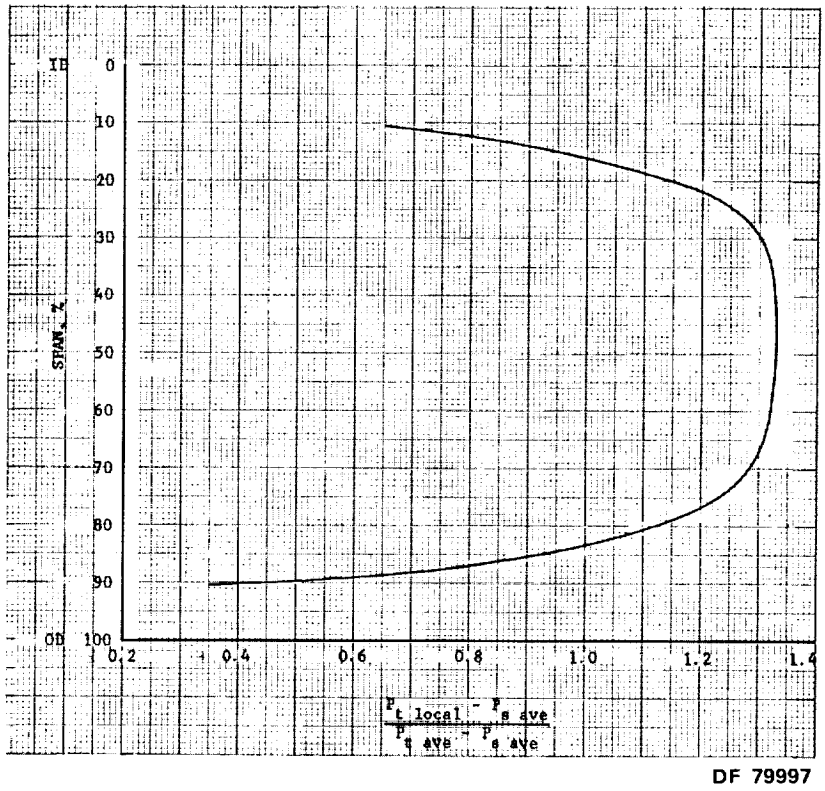

Figure 60. Average Radial Velocity Head Profile, Survey Rake

APPENDIX C

INSTRUMENTATION

Instrumentation was provided to measure the following parameters:

1. Combustor airflow.
2. Fuel flow for each combustion zone (combustor outer and inner annuli and preheater).
3. Fuel temperature and pressure for each zone.
4. Combustor inlet total temperature, total pressure and static pressure.
5. Combustor outlet total temperature and pressure. The outlet static pressure was assumed to be ambient.
6. Miscellaneous diffuser and combustor total and static pressures.

A cross section of the test rig showing the location of the various instrumentation planes is shown in figure 61. A brief description of the instrumentation and monitoring equipment used is described below.

Airflow. - As mentioned in the section on test rig hardware (Appendix B), the combustor airflow was measured with a venturi meter. The inlet total temperature and pressure sensors were located in the flow straightener approximately 12 inches (30.480 cm) upstream of the venturi throat. Two, chromel-alumel, shielded thermocouples spaced 180 degrees (3.141 radians) apart measured total temperature, and two kiel-type pressure probes spaced 180 degrees (3.141 radians) apart measured total pressure. The static pressure at the venturi throat was measured with two wall taps spaced 180 degrees (3.141 radians) apart.

The venturi inlet temperature was monitored on a 0 to 1600°F (255.4 to 1144.3°K) indicating potentiometer, and the total and static pressures on 0- to 80-inch (0- to 2.03-m) mercury filled, U-type manometers.

Fuel Flow. - Fuel flow to each of the three combustion zones was measured by turbine-type flowmeters. The data from these meters were monitored on a 5-channel, preset digital counter. Fuel temperature was measured by a chromel-alumel immersion thermocouple and monitored on an indicating potentiometer. Fuel pressures were measured by wall static pressure taps located in the inlet supply lines and were monitored on 0- to 1000-psig (0- to 699.6-N/cm^2) pressure gages.

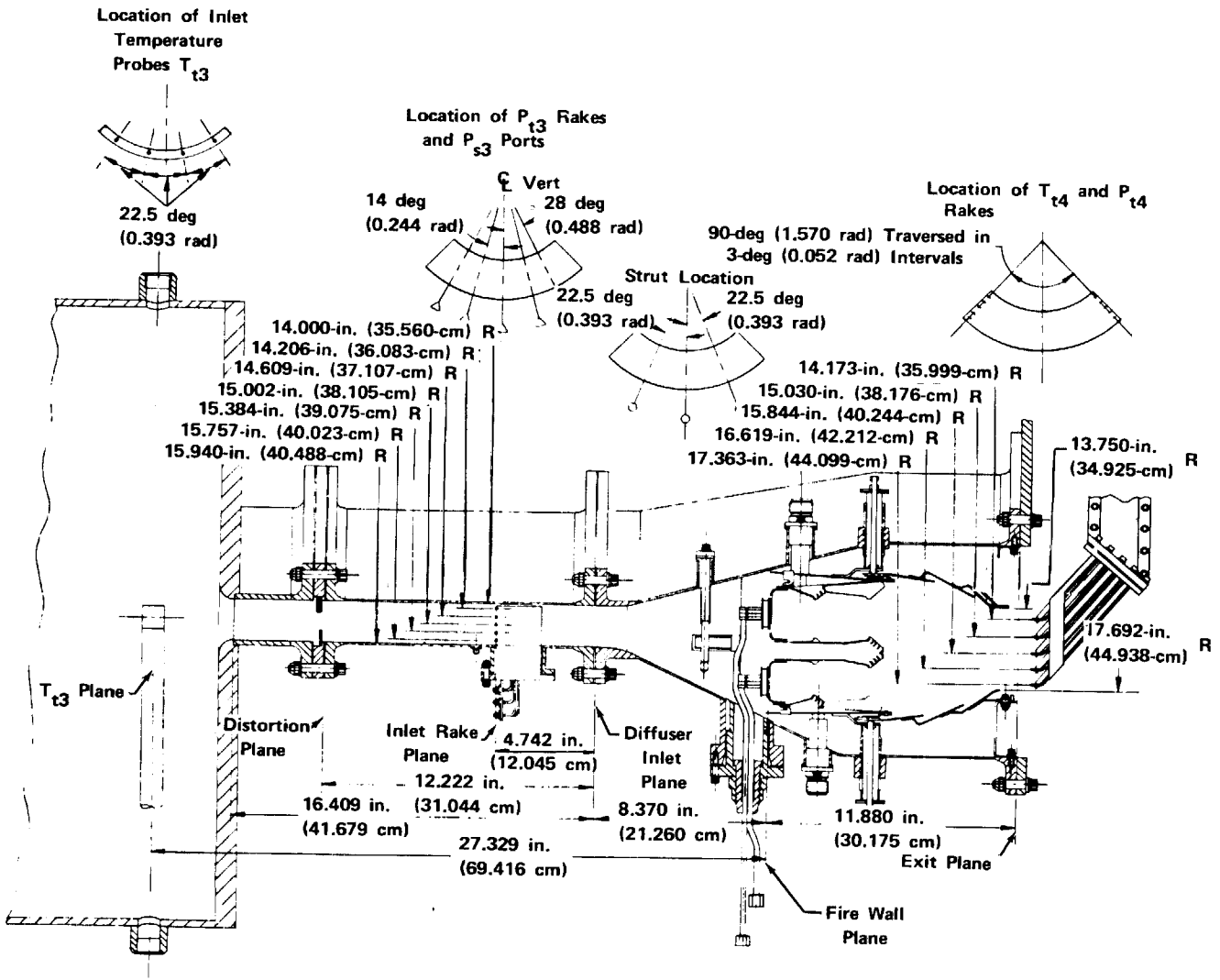

Figure 61. Test Rig Cross Section Showing Instrumentation Planes

FD 36590A

Test Section Inlet. - Instrumentation to measure airflow properties at the test section inlet included:

1. Four, shielded, chromel-alumel thermocouples located as shown in figure 61. Three of these thermocouples were monitored on a 0 to 1600°F (255.4 to 1144.3°K) indicating potentiometer. The fourth thermocouple was channeled into a temperature control unit and functioned as a preheater overtemperature abort system. The control unit was set so that if the preheater outlet temperature exceeded the desired temperature by more than 100°F (55.6°K) the test would be aborted.

2. The test section inlet total pressure was measured by five, 5-point, total pressure rakes (figure 62) located as shown in figure 61. The data from these rakes were monitored on 0- to 80-inch (0- to 2.03-m), water-filled, U-type manometers.

3. The test section inlet static pressure was measured by five wall taps located as shown in figure 61. The data from these sensors were monitored on 0- to 80-inch (0- to 2.03-m), water-filled, U-type manometers.

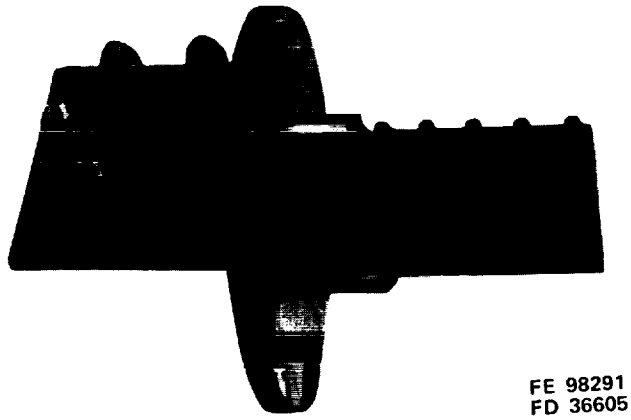

Figure 62. 5-Point Inlet Total Pressure Rake

Combustor Outlet. - Airflow properties at the combustor outlet were measured with a 5-point total temperature and pressure rake (figure 63). Temperature measurements were obtained with aspirated platinum-platinum 10% rhodium thermocouples. A high pressure steam ejector was connected across the probe exhaust to aspirate the thermocouples. The temperature data were taken in 3-degree (0.052-radian) increments across the combustor outlet and were measured on a 0 to 3000°F (255.4 to 1922°K) indicating potentiometer. This potentiometer was equipped with a mercury switch which would abort the test if the thermocouple being monitored exceeded 2700°F (1755°K).

The outlet total pressure was measured by the five 1/8-inch outside diameter tubes shown in figure 63. These tubes were cupped on the end to increase the acceptance angle at which accurate data could be obtained. These pressure data were measured on 0- to 80-inch (0- to 2.03-m), water-filled, U-type manometers.

The outlet static pressure was assumed to be ambient.

Miscellaneous Instrumentation. - Some 73 data channels were provided for measuring various rig pressures such as combustor dome supply pressure, combustion zone pressures, and shroud inlet pressure. These data were monitored on 0- to 80-inch (0- to 2.03-m), water-filled, U-type manometers.

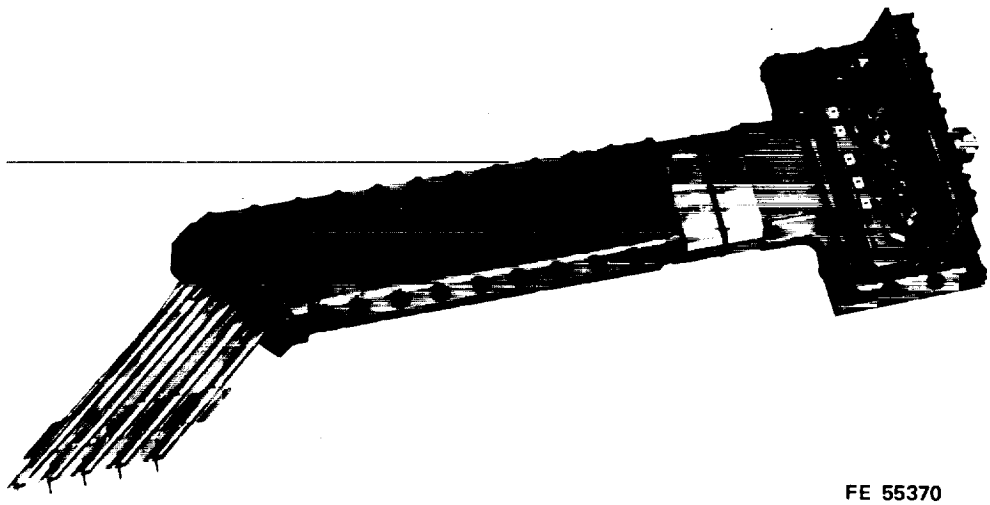

FE 55370
FD 36604

Figure 63. Outlet Total Temperature and Total Pressure Rake

APPENDIX D

EQUIVALENT CONICAL ANGLE

Definition. - The equivalent conical angle (ECA) is defined as the included angle of a conical diffuser that has the same area ratio, inlet area, and wetted surface area as the diffuser under investigation. For annular diffusers, ECA may be approximated by the following equation:

$$ECA = 2 \tan^{-1}\left[\frac{\left(\frac{A_2}{A_1} - 1\right) A_1}{\pi L (R_1 + R_2 + R_3 + R_4)}\right]$$

Where the symbols are defined by:

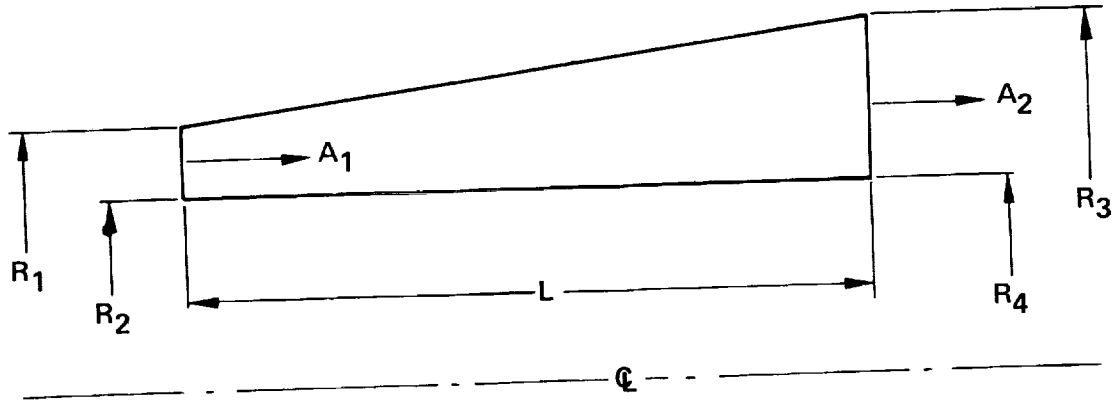

Application. - The above equation for ECA does not consider the presence of struts in the diffusing passage. The equation was used only to arrive at an area ratio for a given ECA and diffusing length assuming that no struts were in the passage. In adding struts, the diffuser wall exit radii were adjusted to maintain the same area ratio.

APPENDIX E

DATA REDUCTION - COMPUTER PROGRAM

LIST OF SYMBOLS

Symbol	Description	Units
A_t	Venturi throat area	$in.^2$
A_{ij}	Elemental flow area at any instrument plane	$in.^2$
C_d	Venturi discharge coefficient	
C_p	Specific heat at constant pressure	$Btu/lb_m °R$
C_v	Specific heat at constant volume	$Btu/lb_m °R$
D_o	Venturi reference diameter	in.
F/A	Fuel/air ratio	$lb_m/sec/lb_m/sec$
g	Gravitational constant	$lb_m\text{-}ft/lb_f\text{-}sec^2$
H	Enthalpy	Btu/hr
J	Energy-work constant	$ft\text{-}lb_f/Btu$
K	Thermal coefficient of expansion	$in./in.°R$
M	Mach number	
P_s	Static pressure	psia
P_t	Total pressure	psia
Q	Heat flux	Btu/hr
R	Gas constant	$ft\text{-}lb_f/lb_m °R$
T_s	Static temperature	°R
T_t	Total temperature	°R
T_o	Venturi reference temperature	°R

Symbol	Description	Units
W_a	Air mass flowrate	lb_m/sec
W_{ext}	External work per unit time	$ft\text{-}lb_f/hr$
W_f	Fuel mass flowrate	lb_m/sec
W_i	Mass flow through incremental flow area	lb_m/sec
W_t	Total mass flowrate	lb_m/sec
W_w	Mass flowrate of water vapor	lb_m/sec
ΔH	Change of enthalpy per unit time	Btu/hr
ΔKE	Change of kinetic energy per unit time	Btu/hr
ΔPE	Change of potential energy per unit time	Btu/hr

Subscripts

a	Dry air
c	Combustion products
HB	Inlet air preheater
i	Incremental area index
i	Circumferential location index
j	Radial location index
MB	Main combustor
mix	Mixture
w	Water vapor
w	Corrector for presents of water vapor
1	Preheater inlet
3	Main combustor inlet
4	Main combustor outlet

This section presents the theoretical principles and assumptions used to determine the performance of the test combustor.

General Assumptions. - The following general assumptions were made in the performance calculations:

1. The perfect gas law ($P_s = \rho RT_s$) applies.
2. Fluid throughout is homogeneous and compressible.
3. All flow processes are isentropic and one-dimensional.
4. Combustion takes place with fuel and dry air; the products of combustion are then assumed to be mixed ideally with the water vapor from the inlet air (see figure 64).

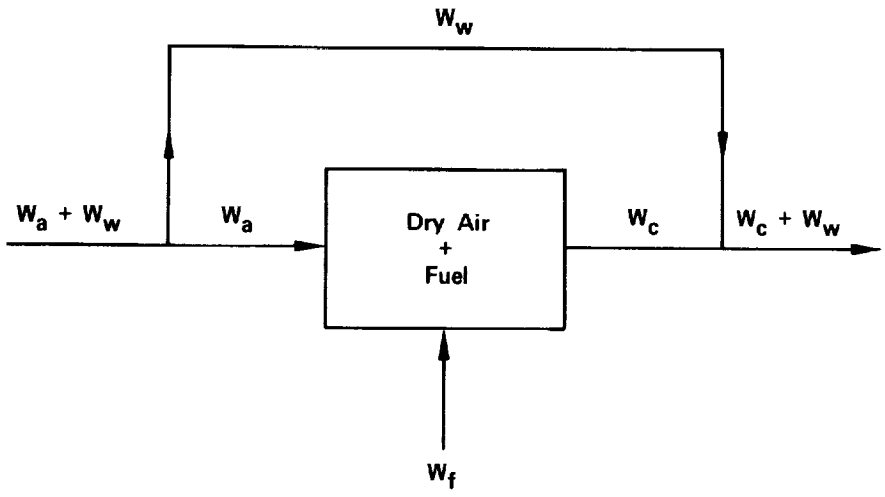

Figure 64. Ideal Combustion Model

Inlet Airflow. - To calculate the inlet air mass flowrate, the specific heat ratio (γ_{mix}) of the inlet air was used. The effect of humidity on this ratio was:

$$\gamma_{mix} = \frac{\gamma_{dry\ air}\,\gamma_{water}\left(C_{P_{dry\ air}} + \frac{w_w}{w_a} C_{P_{water}}\right)}{\gamma_{water}\,C_{P_{dry\ air}} + \frac{w_w}{w_a}\,\gamma_{dry\ air}\,C_{P_{water}}} \qquad \text{(Eq D1)}$$

The venturi airflow was calculated from the relation:

$$w = A_t \sqrt{g} \frac{P_t}{\sqrt{RT_t}} \frac{M\sqrt{\gamma_{mix}}}{\left[1 + \frac{(\gamma_{mix} - 1)M^2}{2}\right]^{\frac{\gamma_{mix}+1}{2(\gamma_{mix}-1)}}} \quad \text{(Eq D2)}$$

The venturi Mach number was determined from the measured static pressure to total pressure ratio. The venturi throat diameter was corrected for thermal expansion from the relation:

$$A_t = C_d \frac{\pi}{4}\left[D_o + KD_o\,(T - T_o)\right]^2 \quad \text{(Eq D3)}$$

Data Averaging. - To account for the effects of profile shape on the averages, the inlet total pressure, the outlet total pressure, and the outlet total temperature were mass weighted. The mass weighted average of any flow property $\bar{X}$ is given by:

$$\bar{X} = \frac{\sum_{i=1}^{n} X_i W_i}{\sum_{i=1}^{n} W_i} \quad \text{(Eq D4)}$$

Where W_i is the mass flow passing through a small incremental area in the data plane under study. Using the equation of continuity and the expressions developed for the isentropic, one-dimensional flow of an ideal gas the above equation was expanded to:

$$\bar{X} = \frac{\sum_{i=1}^{n}\sum_{j=1}^{k} X_{ij} A_{ij} \left[\frac{1}{T_{t_{ij}}}\left\{\left(\frac{P_{t_{ij}}}{P_s}\right)^{\frac{2(\gamma-1)}{\gamma}} - \left(\frac{P_{t_{ij}}}{P_s}\right)^{\frac{\gamma-1}{\gamma}}\right\}\right]^{1/2}}{\sum_{i=1}^{n}\sum_{j=1}^{k} A_{ij} \left[\frac{1}{T_{t_{ij}}}\left\{\left(\frac{P_{t_{ij}}}{P_s}\right)^{\frac{2(\gamma-1)}{\gamma}} - \left(\frac{P_{t_{ij}}}{P_s}\right)^{\frac{\gamma-1}{\gamma}}\right\}\right]^{1/2}} \quad \text{(Eq D5)}$$

The double summation over all values of "i" and "j" was made since circumferential positions are defined by the subscript "i" and radial positions by the subscript "j".

Heater Burner. - Knowing the heater burner exit temperature, the fuel/dry-air ratio, and the hydrogen/carbon mass ratio of the fuel, the specific heat of the combustion products was determined. The specific heat of the water vapor was determined at this temperature. By ideally mixing the products of combustion with the inlet water vapor, the specific heat of the mixture was calculated:

$$C_{p_{mix}} = C_{p_{comb}} \left[\frac{w_t - Xw_a}{w_t}\right] + C_{p_{water}} \left[\frac{Xw_a}{w_t}\right] \quad \text{(Eq D6)}$$

where:

X = specific humidity, lb_m (water)/lb_m (dry air)

The specific heat ratio at the exit of the heater burner was determined from the gas constant (R) of the products:

$$\gamma = \frac{JC_{p_{mix}}}{JC_{p_{mix}} - R} \quad \text{(Eq D7)}$$

The heater burner combustion efficiency was calculated since this efficiency provided a check on airflow measurements, heat loss, and main combustor inlet temperature measurement. This combustion efficiency calculation and the humidity corrections to specific heats and temperatures were the same as those described for the main combustor performance analysis in the following paragraph.

Performance Without Heated Inlet. - Without inlet air heating, the airflow was unaltered in composition before reaching the main combustor inlet. The main combustor fuel/air ratio was:

$$F/A_{MB} = \frac{w_{F_{MB}}}{w_{dry\ air}} \quad \text{(Eq D8)}$$

From the measured main combustor inlet temperature (T_{t3} or T_{in}) the ideal temperature rise across the combustor was obtained.

$$\Delta t_{ideal} = f(T_{in}, F/A, P_c) \quad \text{(Eq D-9)}$$

and,

$$T_{t4\ ideal\ dry} = T_{in} + \Delta t_{ideal} \quad \text{(Eq D10)}$$

The ideal dry exit temperature was corrected due to the humidity present in the inlet air before combustion. To accomplish this, the specific heats at constant pressure of both the water vapor and the combustion products were obtained at the calculated ideal exit temperature for the dry products.

$$R = f(T_{in}, F/A, P_c)$$

$$C_{p4_{dry\ comb\ product}} = f(T_{in}, F/A, P_c)$$

$$C_{p4_{water\ vapor}} = f(T_{t4\ ideal\ dry})$$

By an ideal mixing process,

$$C_{p4_{mix}} = C_{p4_{dry\ comb\ prod}}\left[\frac{w_{t4} - X \cdot w_{dry\ air}}{w_{t4}}\right] + C_{p4_{water\ vapor}}\left[\frac{X \cdot w_{dry\ air}}{w_{t4}}\right] \quad \text{(Eq D11)}$$

The humidity correction to the ideal exit temperature was made as follows:

$$\frac{Q + W_{ext}}{J} = \Delta H + \frac{\Delta KE}{J} + \frac{\Delta PE}{J} + \text{etc.} \quad \text{(Eq 12)}$$

Assuming Q, W_{ext}, ΔKE, ΔPE, etc., were negligible during the mixing process,

$$\Delta H = 0$$

$$H_{in} = H_{out}$$

$$H_{out} = H_{water\ in} + H_{dry\ air} + H_{fuel} = H_{water\ in} + H_{comb\ prod}$$

This is true because energy is assumed to be conserved during combustion of the dry air and fuel.*

Assuming a calorically perfect gas for the mixing process (i.e., constant specific heats):

$$W_{out} C_{p_{out}} T_{out} = w_{water\ in} C_{p_{water\ in}} T_{water\ in} + w_{comb} C_{p_{comb}} T_{comb}$$

$$T_{out} = T_{comb}\left[\frac{C_{p_{comb}}\ w_{comb}}{C_{p_{out}}\ w_{out}}\right] + T_{water\ in}\left[\frac{C_{p_{water}}\ w_{water}}{C_{p_{out}}\ w_{out}}\right]$$

*H_{fuel} includes enthalpy of reaction; therefore,

$$H_{out} = H_{water\ in} + H_{comb\ prod}$$

or,

$$T_{t4_w} = T_{t4_{ideal\ dry}} \left[\frac{C_{p4_{dry\ comb\ prod}}}{C_{p4_{mix}}} \frac{\left(w_{t4} - X \cdot w_{dry\ air}\right)}{w_{t4}} \right] + \cdot T_{in} \left[\frac{C_{p_{water\ vapor}}}{C_{p4_{mix}}} \frac{\left(X \cdot w_{dry\ air}\right)}{w_{t4}} \right]$$

(Eq D13)

The result was the expression for the ideal main combustor temperature with humid air. This temperature was used to determine combustor efficiency as explained on page 11.

Performance With Heated Inlet. - When the heater burner was used to raise the temperature of the inlet air to the main combustor, part of the oxygen in the inlet air was removed in the heater burner and combustion products were added. The fuel/air ratio of the main combustor was corrected for this vitiation effect.

By assuming the combustion of the heater fuel and the main combustor fuel took place together instead of separately, an overall fuel/air ratio was determined.

$$F/A_{overall} = \frac{w_{F_{HB}} + w_{F_{MB}}}{w_{dry\ air}} \qquad \text{(Eq D14)}$$

The ideal main burner exit temperature was determined by a procedure that calculates a fictitious heater burner inlet temperature (T_{t1} fictitious).

$$\Delta t_{overall} = f\left(F/A_{overall}, T_{t1_{fict}}\right) \qquad \text{(Eq D15)}$$

From a curve of ideal temperature rise vs fuel/air ratio, a fictitious temperature rise vs fuel/air ratio for constant main combustor inlet temperatures was plotted. This fictitious rise was the rise that would have occurred if the measured heater burner fuel flow were burned with the resulting heater burner exit temperature equal to the main combustor inlet temperature. The heater burner combustor process and the heat loss between the heater and main combustor inlet were therefore treated in a single process that started at the temperature $T_{t1_{fict}}$.

The main combustor inlet temperature, T_{t3}, was measured during each test. The fictitious heater burner inlet temperature was obtained as follows:

$$F/A_{HB} = \frac{w_{F_{HB}}}{w_{dry\ air}} \cdot$$

$$\Delta t_{fict} = f(F/A_{HB}, T_{t3}) \qquad \text{(Eq D16)}$$

$$T_{t1_{fict}} = T_{t3} - \Delta t_{fict}$$

The ideal rise of the main combustor assuming dry air was then known.

$$\Delta t_{MB_{ideal\ dry}} = \Delta t_{overall} - \Delta t_{fict} \qquad \text{(Eq D17)}$$

The ideal main combustor exit temperature, assuming dry air, was as follows:

$$T_{t4_{ideal\ dry}} = T_{t1_{fict}} + \Delta t_{overall} \qquad \text{(Eq D18)}$$

The expression for the ideal main combustor exit temperature corrected for humid airflow, is the same as the expression obtained for performance without heated inlet.

Procedure for Normalizing Radial Temperature Profile. - To compare the outlet radial temperature profile with a desired radial profile having a mass-weighted average temperature of 2200°F (1477.5°K) a normalizing procedure is needed. The average temperature rise of the desired profile is

$$\Delta TCOR = T_{out_{desired}} - T_{in},\ ^\circ R \qquad \text{(Eq D19)}$$

The average temperature rise for the profile under consideration is:

$$\Delta TAVE = T_{out} - T_{in} \qquad \text{(Eq D20)}$$

Each of the local temperature rises under consideration, when multiplied by the ratio $\Delta TCOR/\Delta TAVE$, will become the local temperature rise that would have resulted from the combustor under consideration if the mass weighted average temperature at the exit had been 2200°F (1477.5°K).

Therefore, the corrected local mass weighted average radial temperature is obtained.

$$TCOR(J) = \Delta TLOC(J) \frac{(\Delta TCOR)}{(\Delta TAVE)} + T_{in} \qquad \text{(Eq D21)}$$

This procedure was used only when the measured average temperature approximated the desired average temperature since the normalizing procedure tends to distort the radial profile.

REFERENCES

1. Kitts, D.L.: "Development of Short-Length Turbojet Combustor," NASA CR-54560, 1968.

2. Chamberlain, John: "The Ram Induction Combustor Concept," presented to the AIAA Third Propulsion Joint Specialist Conference, Washington D.C., 18 July 1967.

3. Rusnak, J.P. and Shadowen, J.H.: "Development of an Advanced Annular Combustor," NASA CR-72453, 1969.

DISTRIBUTION LIST FOR REPORT NO. CR-72734

1. NASA-Lewis Research Center
21000 Brookpark Road
Cleveland, Ohio 44135
Attention:

Report Control Office	MS 5-5	1
Technology Utilization	MS 3-19	1
Library	MS 60-3	2
Fluid Systems Components Division	MS 5-3	1
W. L. Stewart	MS 77-2	1
J. Howard Childs	MS 60-4	1
W. H. Roudebush	MS 60-4	1
L. Schopen	MS 77-3	1
J. B. Esgar	MS 60-4	1
H. H. Ellerbrock	MS 60-4	1
W. T. Olson	MS 3-16	1
R. R. Hibbard	MS 3-5	1
J. F. Dugan, Jr.	MS 501-2	1
Seymour Lieblein	MS 100-1	1
R. E. Jones	MS 60-6	1
Jack Grobman	MS 60-6	1
P. J. Perkins	MS 60-6	10

2. S. C. Fiorello
Aeronautical Engine Laboratory
Naval Air Engineering Center
Philadelphia, Pennsylvania 19112 — 1

3. Aerospace Research Laboratory
Wright-Patterson AFB, Ohio 45433
Attention:
Dr. R. G. Dunn — 1

4. NASA Scientific & Technical Information Facility
P. O. Box 33
College Park, Maryland 20740
Attention:
NASA Representative
RQT-2448 — 6

5. FAA Headquarters
800 Independence Ave. S.W.
Washington, D. C. 20533
Attention:
R. W. Pinnes SS-120
Library — 1

6. NASA Headquarters
600 Independence Ave. S.W.
Washington, D. C. 20546
Attention:
N. F. Rekos (RAP) 1

7. Department of the Army
U.S. Army Aviation Material Laboratory
Propulsion Division (SAUFE-PP)
Fort Eustis, Virginia 23604
Attention:
J. White 1
E. T. Johnson 1

8. United Aircraft of Canada, Ltd
P. O. Box
Lonquenil, Quebec, Canada
Attention:
Miss Mary Cullen 1

9. Air Force Office of Scientific Research
1400 Wilson Boulevard
Arlington, Virginia 22209
Attention:
SREP 1

10. Defense Documentation Center (DDC)
Cameron Station
5010 Duke Street
Alexandria, Virginia 22314 1

11. Department of the Navy
Bureau of Naval Weapons
Washington, D. C. 20025
Attention:
Robert Brown, RAPP14 1

12. Department of the Navy
Bureau of Ships
Washington, D. C. 20360
Attention:
G. L. Graves 1

13. NASA-Langley Research Center
Langley Station
Technical Library
Hampton, Virginia 23365
Attention:
Mark R. Nichols 1
John V. Becker 1

14. United States Air Force
Aero Propulsion Laboratory
Area B, Bldg. 18D
Wright-Patterson A.F.B., Ohio 45433
Attention:

Robert E. Henderson		1

15. United Aircraft Corporation
Pratt & Whitney Aircraft Division
400 Main Street
East Hartford, Connecticut 06108
Attention:

G. Andreini		1
Library		1
R. Marshall		1

16. United Aircraft Research
East Hartford, Connecticut
Attention:

Library		1

17. Allison Division of GMC
Department 8894, Plant 8
P. O. Box 894
Indianapolis, Indiana 46206
Attention:

J. N. Barney		1
G. E. Holbrook		1
Library		1

18. Northern Research & Engineering Corp.
219 Vassar Street
Cambridge, Massachusetts 02139
Attention:

K. Ginwala		1

19. General Electric Company
Flight Propulsion Division
Cincinnati, Ohio 45215
Attention:

J. W. McBride	H-44	1
F. Burggraf	H-32	1
S. N. Suciu	H-32	1
C. Danforth	H-32	1
Technical Information Center	N-32	1
D. Bahr		

20. General Electric Company
1000 Western Avenue
West Lynn, Massachusetts 01905
Attention:

Dr. C. W. Smith		1
Library Building	2-40M	4

21. Curtiss-Wright Corportation
Wright Aeronautical Division
Woodridge, New Jersey 07075
Attention:
D. Wagner 1
W. Walker 1

22. AiResearch Manufacturing Company
402 South 36th Street
Phoenix, Arizona 85034
Attention:
Robert O. Bullock 1

23. AiResearch Manufacturing Company
9851 Sepulveda Boulevard
Los Angeles, California 90009
Attention:
Dr. N. Van Le 1

24. AVCO Corporation
Lycoming Division
550 South Main Street
Stratford, Connecticut 06497
Attention:
Claus W. Bolton 1
Charles Kuintzle 1

25. Continental Aviation & Engineering Corporation
12700 Kercheval
Detroit, Michigan 48215
Attention:
Eli H. Bernstein 1
Howard C. Walch 1

26. International Harvester Company
Solar Division
2200 Pacific Highway
San Diego, California 92112
Attention:
P. A. Pitt 1
Mrs. L. Walper 1

27. Goodyear Atomic Corporation
Box 628
Piketon, Ohio
Attention:
C. O. Langebrake 1

28. George Derderian AIR 53622 B
Department of the Navy
Bureau of Navy
Washington, D. C. 20360 — 1

29. The Boeing Company
Commercial Airplane Division
P. O. Box 3991
Seattle, Washington 98124
Attention:
G. J. Schott — MS 80-66 — 1

30. The Boeing Company
Missile and Information Systems Division
224 N. Wilkinson Street
Dayton, Ohio 45402
Attention:
Warren K. Thorson — 1

31. Aerojet-General Corporation
Sacramento, California 95809
Attention:
M. S. Nylin — 1
Library — 1

32. Cornell Aeronautical Laboratory
4455 Genessee Street
Buffalo 21, New York — 1

33. Marquardt Corporation
16555 Saticoy Street
Van Nuys, California — 1

34. Thompson Ramo Wooldridge
23555 Euclid Avenue
Cleveland, Ohio — 1

35. Aro, Incorporated
Arnold Air Force Station
Tennessee — 1